



Analysis of a Generally Oriented Crack in a Functionally Graded Strip Sandwiched Between Two Homogeneous Half Planes

N. Shbeeb, W.K. Binienda and K. Kreider
The University of Akron, Akron, Ohio

The NASA STI Program Office . . . in Profile

Since its founding, NASA has been dedicated to the advancement of aeronautics and space science. The NASA Scientific and Technical Information (STI) Program Office plays a key part in helping NASA maintain this important role.

The NASA STI Program Office is operated by Langley Research Center, the Lead Center for NASA's scientific and technical information. The NASA STI Program Office provides access to the NASA STI Database, the largest collection of aeronautical and space science STI in the world. The Program Office is also NASA's institutional mechanism for disseminating the results of its research and development activities. These results are published by NASA in the NASA STI Report Series, which includes the following report types:

- **TECHNICAL PUBLICATION.** Reports of completed research or a major significant phase of research that present the results of NASA programs and include extensive data or theoretical analysis. Includes compilations of significant scientific and technical data and information deemed to be of continuing reference value. NASA's counterpart of peer-reviewed formal professional papers but has less stringent limitations on manuscript length and extent of graphic presentations.
- **TECHNICAL MEMORANDUM.** Scientific and technical findings that are preliminary or of specialized interest, e.g., quick release reports, working papers, and bibliographies that contain minimal annotation. Does not contain extensive analysis.
- **CONTRACTOR REPORT.** Scientific and technical findings by NASA-sponsored contractors and grantees.

- **CONFERENCE PUBLICATION.** Collected papers from scientific and technical conferences, symposia, seminars, or other meetings sponsored or cosponsored by NASA.
- **SPECIAL PUBLICATION.** Scientific, technical, or historical information from NASA programs, projects, and missions, often concerned with subjects having substantial public interest.
- **TECHNICAL TRANSLATION.** English-language translations of foreign scientific and technical material pertinent to NASA's mission.

Specialized services that complement the STI Program Office's diverse offerings include creating custom thesauri, building customized data bases, organizing and publishing research results . . . even providing videos.

For more information about the NASA STI Program Office, see the following:

- Access the NASA STI Program Home Page at **<http://www.sti.nasa.gov>**
- E-mail your question via the Internet to **help@sti.nasa.gov**
- Fax your question to the NASA Access Help Desk at (301) 621-0134
- Telephone the NASA Access Help Desk at (301) 621-0390
- Write to:
NASA Access Help Desk
NASA Center for Aerospace Information
7121 Standard Drive
Hanover, MD 21076



Analysis of a Generally Oriented Crack in a Functionally Graded Strip Sandwiched Between Two Homogeneous Half Planes

N. Shbeeb, W.K. Binienda and K. Kreider
The University of Akron, Akron, Ohio

Prepared under Grant NAG3-2069

National Aeronautics and
Space Administration

Glenn Research Center

Acknowledgments

This work was sponsored in part by NASA Glenn Research Center Grant NAG3-2069 and the University of Akron.
The encouragement and support from the program manager, Dr. Gary Halford, of NASA is appreciated.

This report is a formal draft or working paper, intended to solicit comments and ideas from a technical peer group.

This report contains preliminary findings, subject to revision as analysis proceeds.

Available from

NASA Center for Aerospace Information
7121 Standard Drive
Hanover, MD 21076
Price Code: A03

National Technical Information Service
5285 Port Royal Road
Springfield, VA 22100
Price Code: A03

Analysis of a Generally Oriented Crack in a Functionally Graded Strip Sandwiched Between Two Homogeneous Half Planes.

N. Shbeeb, W. K. Binienda and K. Kreider

The University of Akron

Akron, OH 44325-3905

Tel.: (330) 972-6693

Fax: (330) 972-6020

Email: wbininda@uakron.edu

Abstract

The driving forces for a generally oriented crack embedded in a Functionally Graded strip sandwiched between two half planes are analyzed using singular integral equations with Cauchy kernels, and integrated using Lobatto-Chebyshev collocation. Mixed-mode Stress Intensity Factors (SIF) and Strain Energy Release Rates (SERR) are calculated. The Stress Intensity Factors are compared for accuracy with previously published results. Parametric studies are conducted for various non-homogeneity ratios, crack lengths, crack orientation and thickness of the strip. It is shown that the SERR is more complete and should be used for crack propagation analysis.

1. Introduction

One way to reduce the residual stresses in composites is to process fully tailored materials and interfacial zones with predetermined continuously varying mechanical properties. Such materials are known as Functionally Graded Materials (FGM) (see Asish et. al., 1997 and Holt et. al., 1993). Some FGM could be described as two-phase particulate composites where the volume fractions of its constituents differ continuously in the thickness direction (see Niino and Maeda, 1990; Hirano and Yamada, 1988; Hirano et. al., 1988; and Kawasaki and Watanabe R., 1990). This implies that the composition profile could be tailored to give desired thermomechanical properties. One of the most important of these properties is the minimization of crack propagation. In order to design FGM components, then, the driving forces of crack propagation must be fully understood.

The problem under consideration here is that of a generally oriented crack embedded in a nonhomogeneous strip sandwiched between two isotropic half planes. A system of singular integral equations with Cauchy kernels is used to analyze the driving forces (Stress Intensity Factors (SIF) and Strain Energy Release Rates (SERR)) of crack propagation.

The present work is a generalization of a sequence of papers (Delale and Erdogan (1983), (1988a), (1988b), Konda and Erdogan (1994), and Chen and Ergodan (1996)) concerning driving forces of crack propagation for problems involving various boundary conditions and crack geometry. In these papers, an exponential variation in material properties within the FGM is assumed, and it is shown that Poisson's ratio has little effect on stress intensity factors. Therefore, in the present formulation, the same Poisson ratio

is used in all three materials, while the shear modulus has an exponential form. Also, these papers considered only horizontally oriented cracks, while the present paper addresses a crack with arbitrary orientation angle.

The solution methodology follows the basic steps presented in the previous papers. Specifically, the problem is cast in perturbation form. First, the crack surface tractions are computed for an FGM embedded between the two half planes with given far field stresses when no crack is present. In the second step, these tractions are used to compute the stresses at the crack tips for the perturbation problem. These steps are depicted in Figures 1b and 1c. In order to account for the arbitrary orientation angle, the perturbation problem is separated into two parts, depicted in Figures 2b and 2c. The first part includes the influence of the interfaces, and the second part examines the crack in an infinite FGM. Details are shown in the next section.

2. Formulation of the problem

The geometry of the problem is shown in Figure 1a. The two dissimilar materials, which are perfectly bonded to the FGM, are isotropic and homogeneous, the FGM has a finite thickness h , and is denoted as Material 2. Material 1 occupies the lower half plane, for $y < 0$, while Material 3 occupies the upper half plane for $y > h$.

In global coordinates (x, y) , the shear modulus of the FGM is assumed to be as follows:

$$\mu_2(y) = \mu_1 e^{\gamma y} \quad (1)$$

and in local coordinates (x_1, y_1) as:

$$\mu_2(x_1, y_1) = \mu_1 e^{\beta x_1 + \delta y_1} \quad (2)$$

where

$$\begin{aligned} \gamma &= \frac{1}{h} \ln\left(\frac{\mu_3}{\mu_1}\right) \\ \delta &= \gamma \cos(\theta) \\ \beta &= \gamma \sin(\theta) \end{aligned} \quad (3)$$

Hooke's law relates strain and stress using two independent material constants:

$$\begin{aligned} \epsilon_{xx} &= \frac{1}{8\mu} [(\kappa + 1) \sigma_{xx} + (\kappa - 3) \sigma_{yy}] \\ \epsilon_{yy} &= \frac{1}{8\mu} [(\kappa - 3) \sigma_{xx} + (\kappa + 1) \sigma_{yy}] \\ \epsilon_{xy} &= \frac{1}{2\mu} \tau_{xy} \end{aligned} \quad (4)$$

where the bulk modulus, κ , is defined as,

$$\kappa = 3 - 4\nu \quad \text{for} \quad \text{plane strain} \quad (5)$$

or

$$\kappa = \frac{3 - \nu}{1 + \nu} \quad \text{for} \quad \text{plane stress} \quad (6)$$

The solution strategy is shown in Figures 1b and 1c. The governing equation for the half plane is

$$\frac{\partial^4 F_1(x, y)}{\partial x^4} + 2 \frac{\partial^4 F_1(x, y)}{\partial x^2 \partial y^2} + \frac{\partial^4 F_1(x, y)}{\partial y^4} = 0 \quad (7)$$

The solution of (7) is found by applying the Fourier Transform:

$$F_1(x, y) = \int_{-\infty}^{\infty} V(\alpha, y) e^{-ix\alpha} d\alpha \quad (8)$$

and solving the characteristic equation

$$\begin{aligned} \alpha^4 V - 2\alpha^2 \frac{d^2 V}{dy^2} + \frac{d^4 V}{dy^4} &= 0 \\ \Rightarrow m^4 - 2\alpha^2 m^2 + \alpha^4 &= 0 \\ \Rightarrow m_1 = m_3 = |\alpha| \quad \& \quad m_2 = m_4 = -|\alpha| \end{aligned} \quad (9)$$

so that,

$$F_1(x, y) = \frac{1}{2\pi} \int_{-\infty}^{\infty} [(D_1(\alpha) + yD_2(\alpha))e^{|\alpha|y} + (D_3(\alpha) + yD_4(\alpha))e^{-|\alpha|y}] e^{ix\alpha} d\alpha \quad (10)$$

Due to the condition of irregularity at $y < 0$ (the stress function vanishes as $y \rightarrow -\infty$), $D_3(\alpha)$ and $D_4(\alpha)$ must be zero, therefore

$$F_1(x, y) = \frac{1}{2\pi} \int_{-\infty}^{\infty} [(D_1(\alpha) + yD_2(\alpha))e^{|\alpha|y}] e^{ix\alpha} d\alpha \quad (11)$$

Similarly for Material 3, the application of the condition of irregularity at $y > 0$ yields

$$F_3(x, y) = \frac{1}{2\pi} \int_{-\infty}^{\infty} [(C_1(\alpha) + yC_2(\alpha))e^{-|\alpha|y}] e^{i\alpha x} d\alpha \quad (12)$$

The solution strategy of the perturbation problem is shown in Figure 2. The Airy stress function method is adopted in this study, mainly for making use of the technique developed by Delale and Erdogan (1988). It is assumed that the Airy stress function for the FGM is composed of two functions; one is associated with an infinite plane containing the crack on the x_1 -axis, $U_2(x_1, y_1)$ (see Figure 2c), while the second is an uncracked strip, $F_2(x, y)$ (see Figure 2b).

The governing equation in the global coordinate system is

$$\begin{aligned} \nabla^2(\sigma_{xx} + \sigma_{yy}) + \gamma^2 \left[\sigma_{xx} + \frac{\kappa_2 - 3}{\kappa_2 + 1} \sigma_y \right] - 2\gamma \frac{\partial}{\partial y} (\sigma_{xx} + \sigma_{yy}) &= 0 \\ \Rightarrow \nabla^4 F_2(x, y) + \gamma^2 \left[\frac{\partial^2 F_2(x, y)}{\partial y^2} + \frac{\kappa_2 - 3}{\kappa_2 + 1} \frac{\partial^2 F_2(x, y)}{\partial x^2} \right] - 2\gamma \frac{\partial}{\partial y} \nabla^2 F_2(x, y) &= 0 \end{aligned} \quad (13)$$

The characteristic equation of (13) is

$$m^4 - 2\gamma m^3 + (\gamma^2 - 2\alpha^2)m^2 + 2\gamma\alpha^2 m + (\alpha^4 - \alpha^2\gamma^2 \frac{\kappa_2 - 3}{\kappa_2 + 1}) = 0 \quad (14)$$

Four roots of (14) and the stress function are obtained in the following forms:

$$\begin{aligned} m_1 &= \frac{\gamma}{2} - \sqrt{\alpha^2 + \frac{\gamma^2}{4} + i\alpha\gamma \sqrt{\frac{3 - \kappa_2}{\kappa_2 + 1}}} \\ m_2 &= \frac{\gamma}{2} + \sqrt{\alpha^2 + \frac{\gamma^2}{4} + i\alpha\gamma \sqrt{\frac{3 - \kappa_2}{\kappa_2 + 1}}} \\ m_3 &= \frac{\gamma}{2} - \sqrt{\alpha^2 + \frac{\gamma^2}{4} - i\alpha\gamma \sqrt{\frac{3 - \kappa_2}{\kappa_2 + 1}}} \\ m_4 &= \frac{\gamma}{2} + \sqrt{\alpha^2 + \frac{\gamma^2}{4} - i\alpha\gamma \sqrt{\frac{3 - \kappa_2}{\kappa_2 + 1}}} \end{aligned} \quad (15)$$

$$\Rightarrow F_2(x, y) = \frac{1}{2\pi} \int_{-\infty}^{\infty} [A_1(\alpha)e^{m_1 y} + A_2(\alpha)e^{m_2 y} + A_3(\alpha)e^{m_3 y} + A_4(\alpha)e^{m_4 y}] e^{i\alpha x} d\alpha \quad (16)$$

The governing equation in the local crack coordinate system is

$$\begin{aligned}
& \nabla^4 U_2(x_1, y_1) - 2\delta \frac{\partial}{\partial y_1} (\nabla^2 U_2(x_1, y_1)) - 2\beta \frac{\partial}{\partial x_1} (\nabla^2 U_2(x_1, y_1)) + \\
& \frac{8\beta\delta}{1+\kappa_2} \frac{\partial^2 U_2(x_1, y_1)}{\partial x_1 \partial y_1} + \beta^2 \left(\frac{\kappa_2 - 3}{1+\kappa_2} \frac{\partial^2 U_2(x_1, y_1)}{\partial y_1^2} + \frac{\partial^2 U_2(x_1, y_1)}{\partial x_1^2} \right) + \\
& \delta^2 \left(\frac{\partial^2 U_2(x_1, y_1)}{\partial y_1^2} + \frac{\kappa_2 - 3}{1+\kappa_2} \frac{\partial^2 U_2(x_1, y_1)}{\partial x_1^2} \right) = 0
\end{aligned} \tag{17}$$

The characteristic equation of (17) is

$$\begin{aligned}
n^4 - 2\delta n^3 + \left(\beta^2 \frac{\kappa_2 - 3}{\kappa_2 + 1} + \delta^2 - 2\alpha(i\beta + \alpha) \right) n^2 + \alpha\delta \left(\frac{8\beta}{\kappa_2 + 1} i + 2\alpha \right) n \\
+ \alpha^2 \left(\alpha^2 + \delta^2 \frac{3 - \kappa_2}{\kappa_2 + 1} + \beta(2i\alpha - \beta) \right) = 0
\end{aligned} \tag{18}$$

The four roots of (18) are

$$\begin{aligned}
n_1 &= \frac{1}{2} \left(\delta + \beta \sqrt{\frac{3 - \kappa_2}{\kappa_2 + 1}} \right) - \frac{1}{2} \sqrt{\left(\delta + \beta \sqrt{\frac{3 - \kappa_2}{\kappa_2 + 1}} \right)^2 + 4(\alpha^2 + i\alpha \left(\beta - \delta \sqrt{\frac{3 - \kappa_2}{\kappa_2 + 1}} \right))} \\
n_2 &= \frac{1}{2} \left(\delta - \beta \sqrt{\frac{3 - \kappa_2}{\kappa_2 + 1}} \right) - \frac{1}{2} \sqrt{\left(\delta - \beta \sqrt{\frac{3 - \kappa_2}{\kappa_2 + 1}} \right)^2 + 4(\alpha^2 + i\alpha \left(\beta + \delta \sqrt{\frac{3 - \kappa_2}{\kappa_2 + 1}} \right))} \\
n_3 &= \frac{1}{2} \left(\delta + \beta \sqrt{\frac{3 - \kappa_2}{\kappa_2 + 1}} \right) + \frac{1}{2} \sqrt{\left(\delta + \beta \sqrt{\frac{3 - \kappa_2}{\kappa_2 + 1}} \right)^2 + 4(\alpha^2 + i\alpha \left(\beta - \delta \sqrt{\frac{3 - \kappa_2}{\kappa_2 + 1}} \right))} \\
n_4 &= \frac{1}{2} \left(\delta - \beta \sqrt{\frac{3 - \kappa_2}{\kappa_2 + 1}} \right) + \frac{1}{2} \sqrt{\left(\delta - \beta \sqrt{\frac{3 - \kappa_2}{\kappa_2 + 1}} \right)^2 + 4(\alpha^2 + i\alpha \left(\beta + \delta \sqrt{\frac{3 - \kappa_2}{\kappa_2 + 1}} \right))}
\end{aligned} \tag{19}$$

By examining the roots carefully, it can be noticed that n_1 and n_2 are always negative as $\alpha \rightarrow \pm\infty$, while n_3 and n_4 are always positive as $\alpha \rightarrow \pm\infty$. This implies that the stress function can be expressed in the following form:

$$\begin{aligned}
U_2(x_1, y_1) &= \frac{1}{2\pi} \int_{-\infty}^{\infty} [B_1(\alpha) e^{n_1 y_1} + B_2(\alpha) e^{n_2 y_1}] e^{ix_1 \alpha} d\alpha; & y_1 > 0 \\
U_2(x_1, y_1) &= \frac{1}{2\pi} \int_{-\infty}^{\infty} [B_3(\alpha) e^{n_3 y_1} + B_4(\alpha) e^{n_4 y_1}] e^{ix_1 \alpha} d\alpha; & y_1 < 0
\end{aligned} \tag{20}$$

Two constants in the system of equation (20) can be determined by application of the continuity of stresses at $y_1=0$, as follows:

$$\begin{aligned}\frac{\partial U_2(x_1, 0^+)}{\partial y_1} &= \frac{\partial U_2(x_1, 0^-)}{\partial y_1} \\ U_2(x_1, 0^+) &= U_2(x_1, 0^-)\end{aligned}\quad (21)$$

$$\begin{aligned}\Rightarrow B_3(\alpha) &= \frac{n_4 - n_1}{n_4 - n_3} B_1(\alpha) + \frac{n_4 - n_2}{n_4 - n_3} B_2(\alpha) \\ B_4(\alpha) &= \frac{n_1 - n_3}{n_4 - n_3} B_1(\alpha) + \frac{n_2 - n_3}{n_4 - n_3} B_2(\alpha)\end{aligned}\quad (22)$$

The general forms of the stress functions used to generate the stress components due to each problem have been obtained. Next, formulate the stresses for the infinite plate with a crack by differentiating the stress function U_2 (B_1 and B_2 are still functions of α):

$$\begin{aligned}\sigma_{x_1 x_1}^{(U_2)}(x_1, y_1^+) &= \frac{1}{2\pi} \int_{-\infty}^{\infty} [n_1^2 B_1 e^{n_1 y_1} + n_2^2 B_2 e^{n_2 y_1}] e^{ix_1 \alpha} d\alpha \\ \sigma_{y_1 y_1}^{(U_2)}(x_1, y_1^+) &= \frac{-1}{2\pi} \int_{-\infty}^{\infty} \alpha^2 [B_1 e^{n_1 y_1} + B_2 e^{n_2 y_1}] e^{ix_1 \alpha} d\alpha \\ \sigma_{x_1 x_1}^{(U_2)}(x_1, y_1^-) &= \frac{1}{2\pi} \int_{-\infty}^{\infty} [n_3^2 (w_1 B_1 + w_2 B_2) e^{n_3 y_1} + n_4^2 (w_3 B_1 + w_4 B_2) e^{n_4 y_1}] e^{ix_1 \alpha} d\alpha \\ \sigma_{y_1 y_1}^{(U_2)}(x_1, y_1^-) &= \frac{-1}{2\pi} \int_{-\infty}^{\infty} \alpha^2 [(w_1 B_1 + w_2 B_2) e^{n_3 y_1} + (w_3 B_1 + w_4 B_2) e^{n_4 y_1}] e^{ix_1 \alpha} d\alpha \\ w_1 &= \frac{n_1 - n_4}{n_3 - n_4}; w_2 = \frac{n_2 - n_4}{n_3 - n_4}; w_3 = \frac{n_3 - n_1}{n_3 - n_4}; w_4 = \frac{n_3 - n_2}{n_3 - n_4}\end{aligned}\quad (23)$$

The singular integral equations for this class of problems are formulated in terms of two auxiliary functions:

$$\begin{aligned}f_1(x_1) &= \frac{\partial}{\partial x_1} [u_1(x_1, 0^+) - u_1(x_1, 0^-)] \\ f_2(x_1) &= \frac{\partial}{\partial x_1} [v_1(x_1, 0^+) - v_1(x_1, 0^-)]\end{aligned}\quad (24)$$

Notice that the auxiliary functions are valid for any x_1 , but are nonzero only within the crack (a, b).

Using Hooke's law for the stresses given by (23), local strains and displacements can be calculated. For example,

$$\begin{aligned}
\varepsilon_{x_1}^{(U_2)}(x_1, y_1^+) &= \frac{1}{8\mu_2} \frac{1}{2\pi} \int_{-\infty}^{\infty} [(\kappa_2 + 1)(n_1^2 B_1 e^{n_1 y_1} + n_2^2 B_2 e^{n_2 y_1}) \\
&\quad - \alpha^2 (\kappa_2 - 3)(B_1 e^{n_1 y_1} + B_2 e^{n_2 y_1})] e^{ix_1 \alpha} d\alpha \\
\varepsilon_{x_1}^{(U_2)}(x_1, y_1^-) &= \frac{1}{8\mu_2} \frac{1}{2\pi} \int_{-\infty}^{\infty} [(\kappa_2 + 1)(n_3^2 (w_1 B_1 + w_2 B_2) e^{n_3 y_1} + n_4^2 (w_3 B_1 + w_4 B_2) e^{n_4 y_1}) \\
&\quad - \alpha^2 (\kappa_2 - 3)((w_1 B_1 + w_2 B_2) e^{n_3 y_1} + (w_3 B_1 + w_4 B_2) e^{n_4 y_1})] e^{ix_1 \alpha} d\alpha
\end{aligned} \tag{25}$$

Using (25) and first equation of (24) it can be shown that

$$\begin{aligned}
8\mu_1 e^{\beta x_1} f_1(x_1) &= \frac{1}{2\pi} \int_{-\infty}^{\infty} (\kappa_2 + 1)[(n_1^2 - n_3^2 w_1 - n_4^2 w_3) B_1 \\
&\quad + (n_2^2 - n_3^2 w_2 - n_4^2 w_4) B_2] e^{ix_1 \alpha} d\alpha
\end{aligned} \tag{26}$$

The Fourier transform of (26) yields

$$\begin{aligned}
F_1(\alpha) &= h_{11} B_1 + h_{12} B_2 \\
h_{11} &= \frac{\kappa_2 + 1}{8\mu_1} (n_1 - n_3)(n_1 - n_4) \\
h_{12} &= \frac{\kappa_2 + 1}{8\mu_1} (n_2 - n_3)(n_2 - n_4) \\
F_1(\alpha) &= \int_a^b f_1(t) e^{(\beta - i\alpha)t} dt
\end{aligned} \tag{27}$$

In order to determine $f_2(x_1)$, it is necessary to find $v(x_1, y_1)$ by integrating the normal strains in the y direction:

$$\begin{aligned}
v(x_1, y_1^+) &= \frac{1}{8\mu_1} [(\kappa_2 - 3) \frac{1}{2\pi} \int_{-\infty}^{\infty} (\frac{n_1^2}{n_1 - \delta} B_1 e^{n_1 y_1} + \frac{n_2^2}{n_2 - \delta} B_1 e^{n_2 y_1}) e^{ix_1 \alpha} d\alpha \\
&\quad - (\kappa_2 + 1) \frac{1}{2\pi} \int_{-\infty}^{\infty} \alpha^2 (\frac{1}{n_1 - \delta} B_1 e^{n_1 y_1} + \frac{1}{n_2 - \delta} B_1 e^{n_2 y_1}) e^{ix_1 \alpha} d\alpha] \\
&\quad \text{and} \\
v(x_1, y_1^-) &= \frac{1}{8\mu_1} [(\kappa_2 - 3) \frac{1}{2\pi} \int_{-\infty}^{\infty} (\frac{n_3^2}{n_3 - \delta} B_3 e^{n_3 y_1} + \frac{n_4^2}{n_4 - \delta} B_4 e^{n_4 y_1}) e^{ix_1 \alpha} d\alpha \\
&\quad - (\kappa_2 + 1) \frac{1}{2\pi} \int_{-\infty}^{\infty} \alpha^2 (\frac{1}{n_3 - \delta} B_4 e^{n_3 y_1} + \frac{1}{n_4 - \delta} B_4 e^{n_4 y_1}) e^{ix_1 \alpha} d\alpha]
\end{aligned} \tag{28}$$

The constant of integration can be set to zero due to the fact that the plate is fixed at the origin. Differentiating (28) and substituting into second equation of (24), then taking the Fourier transform yields

$$\begin{aligned}
F_2(\alpha) &= h_{21}B_1 + h_{22}B_2 \\
h_{21} &= \frac{i\alpha - \beta}{8\mu_1}(\alpha^2(1 + \kappa_2) - \delta^2(\kappa_2 - 3))\left[\frac{(n_1 - n_3)(n_1 - n_4)}{(\delta - n_1)(\delta - n_3)(\delta - n_4)}\right] \\
h_{22} &= \frac{i\alpha - \beta}{8\mu_1}(\alpha^2(1 + \kappa_2) - \delta^2(\kappa_2 - 3))\left[\frac{(n_2 - n_3)(n_2 - n_4)}{(\delta - n_2)(\delta - n_3)(\delta - n_4)}\right] \\
F_2(\alpha) &= \int_a^b f_2(t)e^{(\beta - i\alpha)t} dt
\end{aligned} \tag{29}$$

Equations (27) and (29) can then be solved for B_1 and B_2 :

$$\begin{aligned}
B_1 &= \frac{F_1(\alpha)h_{22} - F_2(\alpha)h_{12}}{h_{11}h_{22} - h_{21}h_{12}} \\
B_2 &= \frac{-F_1(\alpha)h_{21} + F_2(\alpha)h_{11}}{h_{11}h_{22} - h_{21}h_{12}}
\end{aligned} \tag{30}$$

The stresses at any given point in the cracked FGM strip can be expressed by the sum of stresses obtained from the U_2 and F_2 Airy stress functions, namely:

$$\sigma_{ij}^{(2)}(x_1, y_1) = \sigma_{ij}^{(U_2)}(x_1, y_1) + \sigma_{ij}^{(F_2)}(x_1, y_1) \quad \text{for} \quad (i, j = x_1, y_1) \tag{31}$$

These are expressed in (x, y) or (x_1, y_1) coordinates using the regular stress transformation:

$$\begin{aligned}
\begin{Bmatrix} \sigma_{xx} \\ \sigma_{yy} \\ \tau_{xy} \end{Bmatrix} &= \begin{bmatrix} m^2 & n^2 & -2mn \\ n^2 & m^2 & 2mn \\ mn & -mn & m^2 - n^2 \end{bmatrix} \begin{Bmatrix} \sigma_{x_1x_1} \\ \sigma_{y_1y_1} \\ \tau_{x_1y_1} \end{Bmatrix} \\
m &= \cos(\theta); n = \sin(\theta)
\end{aligned} \tag{32}$$

thus the stresses for the FGM are,

$$\begin{aligned}
\sigma_{xx}^{(2)}(x, y) &= \frac{1}{2\pi} \int_{-\infty}^{\infty} [m_1^2 A_1 e^{m_1 y} + m_2^2 A_2 e^{m_2 y} + m_3^2 A_3 e^{m_3 y} + m_4^2 A_4 e^{m_4 y}] e^{ix\alpha} d\alpha \\
&\quad + \cos(\theta)^2 \frac{1}{2\pi} \int_{-\infty}^{\infty} [n_1^2 B_1 e^{n_1 y_1} + n_2^2 B_2 e^{n_2 y_1}] e^{ix_1 \alpha} d\alpha \\
&\quad - \sin(\theta)^2 \frac{1}{2\pi} \int_{-\infty}^{\infty} \alpha^2 [B_1 e^{n_1 y_1} + B_2 e^{n_2 y_1}] e^{ix\alpha} d\alpha \\
&\quad + 2 \sin(\theta) \cos(\theta) \frac{1}{2\pi} \int_{-\infty}^{\infty} i\alpha [n_1 B_1 e^{n_1 y_1} + n_2 B_2 e^{n_2 y_1}] e^{ix_1 \alpha} d\alpha \\
\sigma_{yy}^{(2)}(x, y) &= -\frac{1}{2\pi} \int_{-\infty}^{\infty} \alpha^2 [A_1 e^{m_1 y} + A_2 e^{m_2 y} + A_3 e^{m_3 y} + A_4 e^{m_4 y}] e^{ix\alpha} d\alpha \\
&\quad + \sin(\theta)^2 \frac{1}{2\pi} \int_{-\infty}^{\infty} [n_1^2 B_1 e^{n_1 y_1} + n_2^2 B_2 e^{n_2 y_1}] e^{ix_1 \alpha} d\alpha \\
&\quad - \cos(\theta)^2 \frac{1}{2\pi} \int_{-\infty}^{\infty} \alpha^2 [B_1 e^{n_1 y_1} + B_2 e^{n_2 y_1}] e^{ix\alpha} d\alpha \\
&\quad - 2 \sin(\theta) \cos(\theta) \frac{1}{2\pi} \int_{-\infty}^{\infty} i\alpha [n_1 B_1 e^{n_1 y_1} + n_2 B_2 e^{n_2 y_1}] e^{ix_1 \alpha} d\alpha \\
\tau_{xy}^{(2)}(x, y) &= -\frac{1}{2\pi} \int_{-\infty}^{\infty} i\alpha [m_1 A_1 e^{m_1 y} + m_2 A_2 e^{m_2 y} + m_3 A_3 e^{m_3 y} + m_4 A_4 e^{m_4 y}] e^{ix\alpha} d\alpha \\
&\quad + \sin(\theta) \cos(\theta) \frac{1}{2\pi} \int_{-\infty}^{\infty} [n_1^2 B_1 e^{n_1 y_1} + n_2^2 B_2 e^{n_2 y_1}] e^{ix_1 \alpha} d\alpha \\
&\quad + \sin(\theta) \cos(\theta) \frac{1}{2\pi} \int_{-\infty}^{\infty} \alpha^2 [B_1 e^{n_1 y_1} + B_2 e^{n_2 y_1}] e^{ix\alpha} d\alpha \\
&\quad - (\cos(\theta)^2 - \sin(\theta)^2) \frac{1}{2\pi} \int_{-\infty}^{\infty} i\alpha [n_1 B_1 e^{n_1 y_1} + n_2 B_2 e^{n_2 y_1}] e^{ix_1 \alpha} d\alpha
\end{aligned} \tag{33}$$

The stresses for Material 1 are

$$\begin{aligned}
\sigma_{xx}^{(1)}(x, y) &= \frac{1}{2\pi} \int_{-\infty}^{\infty} [\alpha^2 (D_1 + yD_2) + 2|\alpha|D_2] e^{|\alpha|y} e^{ix\alpha} d\alpha \\
\sigma_{yy}^{(1)}(x, y) &= -\frac{1}{2\pi} \int_{-\infty}^{\infty} [\alpha^2 (D_1 + yD_2)] e^{|\alpha|y} e^{ix\alpha} d\alpha \\
\tau_{xy}^{(1)}(x, y) &= -\frac{1}{2\pi} \int_{-\infty}^{\infty} i\alpha [|\alpha|(D_1 + yD_2) + D_2] e^{|\alpha|y} e^{ix\alpha} d\alpha
\end{aligned} \tag{34}$$

and for Material 3 are

$$\begin{aligned}
\sigma_{xx}^{(3)}(x, y) &= \frac{1}{2\pi} \int_{-\infty}^{\infty} [\alpha^2 (C_1 + yC_2) - 2|\alpha|C_2] e^{-|\alpha|y} e^{ix\alpha} d\alpha \\
\sigma_{yy}^{(3)}(x, y) &= -\frac{1}{2\pi} \int_{-\infty}^{\infty} [\alpha^2 (C_1 + yC_2)] e^{-|\alpha|y} e^{ix\alpha} d\alpha \\
\tau_{xy}^{(3)}(x, y) &= -\frac{1}{2\pi} \int_{-\infty}^{\infty} i\alpha[-|\alpha|(C_1 + yC_2) + C_2] e^{-|\alpha|y} e^{ix\alpha} d\alpha
\end{aligned} \tag{35}$$

From (33), (34) and (35), it can be seen that there are 10 constants, D_1 , D_2 , C_1 , C_2 , A_1 , A_2 , A_3 , A_4 , B_1 and B_2 (still are functions of α in the Fourier space) which must be determined using 10 boundary conditions. There are eight stress and displacement continuity conditions:

$$\begin{aligned}
\sigma_{yy}^{(1)}(x, 0) &= \sigma_{yy}^{(2)}(x, 0) \\
\sigma_{yy}^{(3)}(x, h) &= \sigma_{yy}^{(2)}(x, h) \\
\tau_{xy}^{(1)}(x, 0) &= \tau_{xy}^{(2)}(x, 0) \\
\tau_{xy}^{(3)}(x, h) &= \tau_{xy}^{(2)}(x, h) \quad \text{for} \quad -\infty < x < \infty \\
u^{(1)}(x, 0) &= u^{(2)}(x, 0) \\
u^{(3)}(x, h) &= u^{(2)}(x, h) \\
v^{(1)}(x, 0) &= v^{(2)}(x, 0) \\
v^{(3)}(x, h) &= v^{(2)}(x, h)
\end{aligned} \tag{36}$$

From (36), the other constants can be expressed in terms of B_1 and B_2 , which in turn are expressed in terms of the two unknown auxiliary functions. The remaining two boundary conditions come from the perturbation problem, namely,

$$\begin{aligned}
\sigma_{y_1 y_1}(x_1, 0) &= -p_1(x_1) \quad \text{for} \quad a < x_1 < b \\
\tau_{x_1 y_1}(x_1, 0) &= -p_2(x_1) \quad \text{for} \quad a < x_1 < b
\end{aligned} \tag{37}$$

Here, p_1 and p_2 are the traction forces on the crack surfaces. D_1 , D_2 , C_1 and C_2 are found in terms of A_1 , A_2 , A_3 , A_4 , B_1 and B_2 by using the stress continuity conditions of (36). Further, by using the displacement continuity conditions of (36), the following linear system can be constructed:

$$\begin{bmatrix} C_{11} & C_{12} & C_{13} & C_{14} \\ C_{21} & C_{22} & C_{23} & C_{24} \\ C_{31} & C_{32} & C_{33} & C_{34} \\ C_{41} & C_{42} & C_{43} & C_{44} \end{bmatrix} \begin{bmatrix} A_1 \\ A_2 \\ A_3 \\ A_4 \end{bmatrix} = \begin{bmatrix} J_1 \\ J_2 \\ J_3 \\ J_4 \end{bmatrix} \quad (38)$$

where $D_1, D_2, C_1, C_2, C_{11}$ through C_{44} and J_1 through J_4 are functions of α derived using MATHEMATICA, see Shbeeb (1998).

The system of equations (38) can be solved for A_i , ($i=1,..,4$) in terms of the unknowns $F_1(\alpha)$ and $F_2(\alpha)$, which are components of J_i , ($i=1..4$) as follows:

$$A_i = \sum_{j=1}^4 \frac{Q_{ij}}{Q} J_j \quad i = 1 \dots 4 \quad (39)$$

Here, Q is the determinant of the 4 by 4 coefficient matrix and the Q_{ij} are the corresponding 3 by 3 cofactors.

To make use of (37), the stresses of the FGM must be formulated in (x_1, y_1) coordinates as

$$\begin{aligned} \sigma_{y_1 y_1}^{(2)}(x_1, y_1) = & -\frac{1}{2\pi} \int_{-\infty}^{\infty} \alpha^2 (B_1 e^{n_1 y_1} + B_2 e^{n_2 y_1}) e^{ix_1 \alpha} d\alpha \\ & + \frac{1}{2\pi} \int_{-\infty}^{\infty} \left[\sum_{n=1}^4 (m_n \sin(\theta) + i\alpha \cos(\theta))^2 A_n e^{m_n y} \right] e^{ix\alpha} d\alpha \end{aligned} \quad (40)$$

$$\begin{aligned} \tau_{x_1 y_1}^{(2)}(x_1, y_1) = & -\frac{1}{2\pi} \int_{-\infty}^{\infty} i\alpha (n_1 B_1 e^{n_1 y_1} + n_2 B_2 e^{n_2 y_1}) e^{ix_1 \alpha} d\alpha \\ & - \frac{1}{2\pi} \int_{-\infty}^{\infty} \left[\sum_{n=1}^4 ((\alpha^2 + m_n^2) \sin(\theta) \cos(\theta) \right. \\ & \left. + i\alpha m_n (\cos(\theta)^2 - \sin(\theta)^2)) A_n e^{m_n h} \right] e^{ix\alpha} d\alpha \end{aligned} \quad (41)$$

Each term in (40) and (41) must be examined for singular behavior. Upon substitution of (30), (27) and (29) into (40), the first integral above can be written as follows:

$$(\sigma_{y_1 y_1}^{(2)}(x_1, y_1))^{(1)} = -\frac{1}{2} \int_a^b f_1(t) e^{\beta t} k_{11}^{(1)}(x_1, t) dt - \frac{1}{2} \int_a^b f_2(t) e^{\beta t} k_{12}^{(1)}(x_1, t) dt \quad (42)$$

where

$$k_{11}^{(1)}(x_1, t) = \frac{1}{\pi} \int_{-\infty}^{\infty} \alpha^2 \frac{h_{22} e^{n_1 y_1} - h_{21} e^{n_2 y_1}}{h_{11} h_{22} - h_{12} h_{21}} e^{i\alpha(x_1 - t)} d\alpha \quad (43)$$

$$k_{12}^{(2)}(x_1, t) = \frac{1}{\pi} \int_{-\infty}^{\infty} \alpha^2 \frac{h_{11} e^{n_1 y_1} - h_{12} e^{n_2 y_1}}{h_{11} h_{22} - h_{12} h_{21}} e^{i\alpha(x_1 - t)} d\alpha \quad (44)$$

Since the integrands are continuous functions of α and vanish at $\alpha=0$, then any singularity must occur as α goes to infinity. The integrand of (43) vanishes as $\alpha \rightarrow \pm\infty$, while that of (44) is as follows:

$$\frac{h_{11} e^{n_1 y_1} - h_{12} e^{n_2 y_1}}{h_{11} h_{22} - h_{12} h_{21}} \rightarrow \left(\frac{h_{11} - h_{12}}{h_{11} h_{22} - h_{12} h_{21}} \right) e^{-|\alpha| y_1} \rightarrow \mp \frac{2i e^{-\alpha y_1}}{\alpha^2 (\kappa_2 + 1)} \quad \alpha \rightarrow \pm\infty$$

By subtracting and adding this asymptotic value from (44) and taking the limit as y_1 goes to zero, the following is produced:

$$k_{12}^{(1)}(x_1, t) = \frac{1}{\pi} \left[\int_{-\infty}^0 \alpha^2 \left(\frac{h_{11} - h_{12}}{h_{11} h_{22} - h_{12} h_{21}} - \frac{2i}{\alpha^2 (\kappa_2 + 1)} \right) e^{i\alpha(x_1 - t)} d\alpha + \int_0^{\infty} \alpha^2 \left(\frac{h_{11} - h_{12}}{h_{11} h_{22} - h_{12} h_{21}} + \frac{2i}{\alpha^2 (\kappa_2 + 1)} \right) e^{i\alpha(x_1 - t)} d\alpha + \text{SIP} \right] \quad (45)$$

where

$$\text{SIP} = \lim_{y_1 \rightarrow 0} \left(\int_{-\infty}^0 \frac{2i e^{\alpha y_1}}{(\kappa_2 + 1)} e^{i\alpha(x_1 - t)} d\alpha - \int_0^{\infty} \frac{2i e^{-\alpha y_1}}{(\kappa_2 + 1)} e^{i\alpha(x_1 - t)} d\alpha \right) \quad (46)$$

Let $\alpha' = -\alpha$ in the first integral in (46) to obtain

$$\begin{aligned} -\frac{4}{(\kappa_2 + 1)} \lim_{y_1 \rightarrow 0} \int_0^{\infty} e^{-\alpha y_1} \sin(\alpha(t - x_1)) d\alpha &= -\frac{4}{(\kappa_2 + 1)} \lim_{y_1 \rightarrow 0} \frac{t - x_1}{(t - x_1)^2 + y_1^2} \\ &= -\frac{4}{(\kappa_2 + 1)} \frac{1}{t - x_1} \end{aligned} \quad (47)$$

and

$$\begin{aligned} \Rightarrow k_{12}^{(1)}(x_1, t) &= \frac{1}{\pi} \left[\int_{-\infty}^0 \alpha^2 \left(\frac{h_{11} - h_{12}}{h_{11} h_{22} - h_{12} h_{21}} - \frac{2i}{\alpha^2 (\kappa_2 + 1)} \right) e^{i\alpha(x_1 - t)} d\alpha + \int_0^{\infty} \alpha^2 \left(\frac{h_{11} - h_{12}}{h_{11} h_{22} - h_{12} h_{21}} + \frac{2i}{\alpha^2 (\kappa_2 + 1)} \right) e^{i\alpha(x_1 - t)} d\alpha - \frac{4}{(\kappa_2 + 1)} \frac{1}{t - x_1} \right] \end{aligned} \quad (48)$$

Similarly, let $\alpha' = -\alpha$ in (48). Note that every odd power of α becomes negative.

$$\begin{aligned} \Rightarrow k_{12}^{(1)}(x_1, t) = & \frac{1}{\pi} \left[\int_0^\infty \left\{ \alpha^2 \left[\frac{H_{11} - H_{12}}{H_{11}H_{22} - H_{12}H_{21}} + \frac{h_{11} - h_{12}}{h_{11}h_{22} - h_{12}h_{21}} \right] \cos(\alpha(t - x_1)) \right. \right. \\ & + i\alpha^2 \left[\frac{H_{11} - H_{12}}{H_{11}H_{22} - H_{12}H_{21}} + \frac{h_{11} - h_{12}}{h_{11}h_{22} - h_{12}h_{21}} \right. \\ & \left. \left. - \frac{4i}{\alpha^2(\kappa_2 + 1)} \right] \sin(\alpha(t - x_1)) \right\} d\alpha - \frac{4}{(\kappa_2 + 1)} \frac{1}{t - x_1} \right] \end{aligned} \quad (49)$$

The H_{ij} ($i, j=1,2$) have the same forms as the h_{ij} , with the only difference being in the sign of the odd powers of α where they are negative. It is worth noting that:

$$\frac{H_{11} - H_{12}}{H_{11}H_{22} - H_{12}H_{21}} = \text{conjugate}\left(\frac{h_{11} - h_{12}}{h_{11}h_{22} - h_{12}h_{21}}\right) \quad (50)$$

Repeating the same procedure for (43) by splitting the integral in the same manner as in (48) and substituting the result along with (49) into (42) yields the following:

$$\begin{aligned} \lim_{y_1 \rightarrow 0} (\sigma_{y_1 y_1}^{(2)}(x_1, y_1))^{(1)} = & \frac{\mu_1 e^{\beta x_1}}{2} \left[\frac{4}{\pi(\kappa_2 + 1)} \int_a^b \frac{f_2(t)}{t - x_1} dt + \frac{1}{\pi} \int_a^b f_1(t) K_{11}^1(x_1, t) dt \right. \\ & \left. + \frac{1}{\pi} \int_a^b f_2(t) K_{12}^1(x_1, t) dt \right] \end{aligned} \quad (51)$$

where

$$\begin{aligned} K_{11}^{(1)}(x_1, t) = & - \int_0^\infty \left\{ \alpha^2 [X_{11} + \text{conj}(X_{11})] \cos(\alpha(t - x_1)) \right. \\ & \left. + i\alpha^2 [-X_{11} + \text{conj}(X_{11})] \sin(\alpha(t - x_1)) \right\} d\alpha \\ K_{12}^{(1)}(x_1, t) = & - \int_0^\infty \left\{ \alpha^2 [X_{12} + \text{conj}(X_{12})] \cos(\alpha(t - x_1)) \right. \\ & \left. + i\alpha^2 [-X_{12} + \text{conj}(X_{12}) - \frac{4i}{\alpha^2(\kappa_2 + 1)}] \sin(\alpha(t - x_1)) \right\} d\alpha \end{aligned} \quad (52)$$

$$X_{11} = \left(\frac{h_{22} - h_{21}}{h_{11}h_{22} - h_{12}h_{21}} \right)$$

$$X_{12} = \left(\frac{h_{11} - h_{12}}{h_{11}h_{22} - h_{12}h_{21}} \right)$$

The same procedure can be repeated for the first part of the shear stress (41) to obtain

$$\begin{aligned} \lim_{y_1 \rightarrow 0} (\tau_{y_1 y_1}^2(x_1, y_1))^1 &= \frac{\mu_1 e^{\beta x_1}}{2} \left[\frac{4}{\pi(\kappa_2 + 1)} \int_a^b \frac{f_1(t)}{t - x_1} dt + \frac{1}{\pi} \int_a^b f_1(t) K_{21}^1(x_1, t) dt \right. \\ &\quad \left. + \frac{1}{\pi} \int_a^b f_2(t) K_{22}^1(x_1, t) dt \right] \end{aligned} \quad (53)$$

where

$$\begin{aligned} K_{21}^{(1)}(x_1, t) &= - \int_0^\infty \{ i\alpha [X_{21} - \text{conj}(X_{21})] \cos(\alpha(t - x_1)) \\ &\quad + \alpha [X_{21} + \text{conj}(X_{21}) + \frac{4i}{\alpha(\kappa_2 + 1)}] \sin(\alpha(t - x_1)) \} d\alpha \\ K_{22}^{(1)}(x_1, t) &= - \int_0^\infty \{ i\alpha [X_{22} - \text{conj}(X_{22})] \cos(\alpha(t - x_1)) \\ &\quad + \alpha [X_{22} + \text{conj}(X_{22})] \sin(\alpha(t - x_1)) \} d\alpha \\ X_{21} &= \left(\frac{n_1 h_{22} - n_2 h_{21}}{h_{11} h_{22} - h_{12} h_{21}} \right) \\ X_{22} &= \left(\frac{n_2 h_{11} - n_1 h_{12}}{h_{11} h_{22} - h_{12} h_{21}} \right) \end{aligned} \quad (54)$$

The examination of the remaining two parts of the stress equations (40) and (41) and application of the asymptotic expansion and the limit as y_1 goes to zero yields the following terms:

$$\lim_{y_1 \rightarrow 0} (\sigma_{y_1 y_1}^{(2)}(x_1, y_1))^{(2)} = \frac{\mu_1 e^{\beta x_1}}{2} \left[\frac{1}{\pi} \int_a^b f_1(t) K_{11}^{(2)}(x_1, t) dt + \frac{1}{\pi} \int_a^b f_2(t) K_{12}^{(2)}(x_1, t) dt \right] \quad (55)$$

$$\lim_{y_1 \rightarrow 0} (\sigma_{y_1 y_1}^{(2)}(x_1, y_1))^{(2)} = \frac{\mu_1 e^{\beta x_1}}{2} \left[\frac{1}{\pi} \int_a^b f_1(t) K_{11}^{(2)}(x_1, t) dt + \frac{1}{\pi} \int_a^b f_2(t) K_{12}^{(2)}(x_1, t) dt \right] \quad (56)$$

where

$$\begin{aligned}
K_{11}^{(2)}(x_1, t) = & \int_0^\infty \{ [Y_{11} + conj(Y_{11})] \cos[\alpha \cos(\theta)(t - x_1)] \\
& + i[-Y_{11} + conj(Y_{11})] \sin[\alpha \cos(\theta)(t - x_1)] \} d\alpha + \\
& \left(\frac{2a_{11}(x_1^2 \sin(\theta)^2 - \cos(\theta)^2(t - x_1)^2) + 4b_{11}(x_1(t - x_1) \sin(\theta) \cos(\theta))}{(x_1^2 \sin(\theta)^2 + \cos(\theta)^2(t - x_1)^2)^2} + \right. \\
& \left. \frac{2c_{11}x_1 \sin(\theta) + 2d_{11} \cos(\theta)(t - x_1)}{x_1^2 \sin(\theta)^2 + \cos(\theta)^2(t - x_1)^2} \right)
\end{aligned} \tag{57}$$

$$\begin{aligned}
K_{12}^{(2)}(x_1, t) = & \int_0^\infty \{ [Y_{12} + conj(Y_{12})] \cos[\alpha \cos(\theta)(t - x_1)] \\
& + i[-Y_{12} + conj(Y_{12})] \sin[\alpha \cos(\theta)(t - x_1)] \} d\alpha + \\
& \left(\frac{2a_{12}(x_1^2 \sin(\theta)^2 - \cos(\theta)^2(t - x_1)^2) + 4b_{12}(x_1(t - x_1) \sin(\theta) \cos(\theta))}{(x_1^2 \sin(\theta)^2 + \cos(\theta)^2(t - x_1)^2)^2} + \right. \\
& \left. \frac{2c_{12}x_1 \sin(\theta) + 2d_{12} \cos(\theta)(t - x_1)}{x_1^2 \sin(\theta)^2 + \cos(\theta)^2(t - x_1)^2} \right)
\end{aligned}$$

$$\begin{aligned}
K_{11}^{(2)}(x_1, t) = & \int_0^\infty \{ [Y_{11} + conj(Y_{11})] \cos[\alpha \cos(\theta)(t - x_1)] \\
& + i[-Y_{11} + conj(Y_{11})] \sin[\alpha \cos(\theta)(t - x_1)] \} d\alpha + \\
& \left(\frac{2a_{11}(x_1^2 \sin(\theta)^2 - \cos(\theta)^2(t - x_1)^2) + 4b_{11}(x_1(t - x_1) \sin(\theta) \cos(\theta))}{(x_1^2 \sin(\theta)^2 + \cos(\theta)^2(t - x_1)^2)^2} + \right. \\
& \left. \frac{2c_{11}x_1 \sin(\theta) + 2d_{11} \cos(\theta)(t - x_1)}{x_1^2 \sin(\theta)^2 + \cos(\theta)^2(t - x_1)^2} \right)
\end{aligned} \tag{58}$$

$$\begin{aligned}
K_{12}^{(2)}(x_1, t) = & \int_0^\infty \{ [Y_{12} + conj(Y_{12})] \cos[\alpha \cos(\theta)(t - x_1)] \\
& + i[-Y_{12} + conj(Y_{12})] \sin[\alpha \cos(\theta)(t - x_1)] \} d\alpha + \\
& \left(\frac{2a_{12}(x_1^2 \sin(\theta)^2 - \cos(\theta)^2(t - x_1)^2) + 4b_{12}(x_1(t - x_1) \sin(\theta) \cos(\theta))}{(x_1^2 \sin(\theta)^2 + \cos(\theta)^2(t - x_1)^2)^2} + \right. \\
& \left. \frac{2c_{12}x_1 \sin(\theta) + 2d_{12} \cos(\theta)(t - x_1)}{x_1^2 \sin(\theta)^2 + \cos(\theta)^2(t - x_1)^2} \right)
\end{aligned}$$

where Y_{ij} a_{ij} , b_{ij} , c_{ij} can be found in Shbeeb (1998).

By substituting these expressions into (40) and (41), the final system of singular equation is formulated:

$$\begin{aligned}\frac{\kappa_2 + 1}{2\mu_1} e^{-\beta x_1} (-p_1(x_1)) &= \frac{1}{\pi} \int_a^b \frac{f_2(t)}{t - x_1} dt + \frac{1}{\pi} \int_a^b f_1(t) K_{11}(x_1, t) + \frac{1}{\pi} \int_a^b f_2(t) K_{12}(x_1, t) \\ \frac{\kappa_2 + 1}{2\mu_1} e^{-\beta x_1} (-p_2(x_1)) &= \frac{1}{\pi} \int_a^b \frac{f_1(t)}{t - x_1} dt + \frac{1}{\pi} \int_a^b f_1(t) K_{21}(x_1, t) + \frac{1}{\pi} \int_a^b f_2(t) K_{22}(x_1, t)\end{aligned}\quad (59)$$

where,

$$\begin{aligned}K_{11}(x_1, t) &= \frac{\kappa_2 + 1}{4} (K_{11}^{(1)}(x_1, t) + K_{11}^{(2)}(x_1, t)) \\ K_{12}(x_1, t) &= \frac{\kappa_2 + 1}{4} (K_{12}^{(1)}(x_1, t) + K_{12}^{(2)}(x_1, t)) \\ K_{21}(x_1, t) &= \frac{\kappa_2 + 1}{4} (K_{21}^{(1)}(x_1, t) + K_{21}^{(2)}(x_1, t)) \\ K_{22}(x_1, t) &= \frac{\kappa_2 + 1}{4} (K_{22}^{(1)}(x_1, t) + K_{22}^{(2)}(x_1, t))\end{aligned}$$

3. Solution of Singular Integral Equations

The singular integral equations (59) with the Cauchy kernels are solved for the unknown auxiliary functions, $f_1(t)$ and $f_2(t)$, by transforming them into a system of linear algebraic equations. In order to obtain unique results, the following conditions need to be incorporated with the solution:

$$\int_a^b f_i(t) dt = 0 \quad i = 1, 2 \quad (60)$$

The singular integral equation (59) can be solved using Gaussian quadrature. For example, using Lobatto-Chebyshev collocation as described in Theocaris and Ioakimidis (1977), we obtain the system of algebraic equations in terms of discrete unknowns $g(t_k)$ in the following form:

$$\sum_{j=1}^N \frac{b_{ij}}{\pi} \sum_{k=1}^n \frac{g_j(t_k) w_k}{t_k - x_p} + \sum_{j=1}^N \sum_{k=1}^n k_{ij}(x_p, t_k) g_j(t_k) w_k + R_n(x_p) = f_i(x_p) \quad (61)$$

where $p=1, \dots, n$, the w_k are the weights, the abscissas t_k are the roots of the related orthogonal polynomial, and R_n is the error. The abscissas are

$$t_k = \cos\left(\frac{(k-1)\pi}{n-1}\right) \quad k = 1, \dots, n. \quad (62)$$

The corresponding weights are

$$w_1 = w_n = \frac{\pi}{2(n-1)}; w_r = \frac{\pi}{n-1} \quad r = 2, \dots, n-1. \quad (63)$$

The collocation points are

$$x_p = \cos\left(\frac{(2p-1)\pi}{2n-2}\right) \quad p = 1, \dots, n-1. \quad (64)$$

Two additional equations are needed, which are generated using (60) in the following form:

$$\sum_{k=1}^n g_1(s_k) w_k = 0 \quad (65)$$

$$\sum_{k=1}^n g_2(s_k) w_k = 0 \quad (66)$$

By combining (61), (65) and (66), the system of equations can be represented as follows:

$$[A]_{2n \times 2n} \{g\}_{2n} = \{P\}_{2n} \quad (67)$$

This system can be solved by any standard method. Formally, the unknowns are

$$\{g\} = [A]^{-1} \{P\} \quad (68)$$

Finally, the goal is to obtain the SIF in terms of $g_1(t)$ and $g_2(t)$. The SIF are defined as follows:

$$\begin{aligned} k_1(a) &= \lim_{x_1 \rightarrow a} \sqrt{2(a-x_1)} \sigma_{y_1 y_1}(x_1, 0) \\ k_1(b) &= \lim_{x_1 \rightarrow b} \sqrt{2(x_1-b)} \sigma_{y_1 y_1}(x_1, 0) \\ k_2(a) &= \lim_{x_1 \rightarrow a} \sqrt{2(a-x_1)} \tau_{x_1 y_1}(x_1, 0) \\ k_2(b) &= \lim_{x_1 \rightarrow b} \sqrt{2(x_1-b)} \tau_{x_1 y_1}(x_1, 0) \end{aligned} \quad (69)$$

From the principal part the expressions for $g_1(t)$ and $g_2(t)$, Muskhelishvili (1953), the following is obtained for $k_1(a)$:

$$k_1(a) = \frac{2\sqrt{2}\mu_1}{(\kappa_2 + 1)\sqrt{b-a}} e^{\beta a} g_2(a) \quad (70)$$

Similarly,

$$k_1(b) = -\frac{2\sqrt{2}\mu_1}{(\kappa_2 + 1)\sqrt{b-a}} e^{\beta b} g_2(b) \quad (71)$$

$$k_2(a) = \frac{2\sqrt{2}\mu_1}{(\kappa_2 + 1)\sqrt{b-a}} e^{\beta a} g_1(a) \quad (72)$$

$$k_2(b) = -\frac{2\sqrt{2}\mu_1}{(\kappa_2 + 1)\sqrt{b-a}} e^{\beta b} g_1(b) \quad (73)$$

Note that $a=-1$ and $b=1$ when solving (68).

The strain energy release rate (SERR) can be calculated from Erdogan and Konda (1994). They are

$$\begin{aligned} G_1(a) &= \frac{\pi(\kappa_2 + 1)}{8\mu_2(a,0)} k_1(a)^2 \\ G_1(b) &= \frac{\pi(\kappa_2 + 1)}{8\mu_2(b,0)} k_1(b)^2 \\ G_2(a) &= \frac{\pi(\kappa_2 + 1)}{8\mu_2(a,0)} k_2(a)^2 \\ G_2(b) &= \frac{\pi(\kappa_2 + 1)}{8\mu_2(b,0)} k_2(b)^2 \end{aligned} \quad (74)$$

where G_1 is the opening mode SERR and G_2 is the sliding mode SERR. The total SERR is expressed as

$$\begin{aligned} G_T(a) &= \frac{\pi(\kappa_2 + 1)}{8\mu_2(a,0)} (k_1(a)^2 + k_2(a)^2) \\ G_T(b) &= \frac{\pi(\kappa_2 + 1)}{8\mu_2(b,0)} (k_1(b)^2 + k_2(b)^2) \end{aligned} \quad (75)$$

The verification of the solution above is accomplished by comparing the results of this model with that of Erdogan and Konda (1994). In this model, h is set to ∞ to

simulate an infinite FGM plate, with various values of γ_c . The two models give virtually identical results, as seen in Table 1. For $\gamma=0$ (the homogeneous case), the singular integral equations can be reduced to a closed form solution (see for example Tada et. al. (1973)) producing SIF proportional to normal and shear tractions applied on the crack surface.

4. Parametric Studies

The focus of the following parametric study is limited to investigating the influence of the material properties of the half planes, crack length and orientation, and thickness of the FGM interface on the resulting driving force as measured by the SIF and SERR. To accomplish this, the normalized nonhomogeneity constant $\gamma_h = \ln(\mu_3/\mu_1)$ is defined using (3). The range of the constant is assumed to be between -3 and 3 , which includes all known engineering materials. A negative γ_h represents a problem where the bottom half plane is stiffer than the upper half plane. A positive γ_h represents a problem where the upper half plane is stiffer than the lower half plane. Hence, if the shear moduli of all three phases are normalized with respect to μ_1 , the equivalent variation of the shear modulus of the upper half plane takes values of approximately 0.05 to 20 times the lower half plane shear modulus.

In this study, all the cases were considered under plane stress conditions with Poisson's ratio = 0.3 and the materials were subjected to far field normal stress in the y direction. The length of the crack is chosen to be $2c$, and the thickness of the interface is h . All geometrical dimensions are normalized with respect to c or h . Results are presented for the normalized mode-I and mode-II SIF, i.e., k_1/k_0 and k_2/k_0 , and normalized SERR, i.e., G_1/G_0 and G_2/G_0 , where $k_0 = \sigma_{yy}(c)^{1/2}$ and $G_0 = k_0^2 \pi(\kappa+1)/8\mu_1$.

In the first study, consider the influence of the thickness of the interface h/c and non-homogeneity constant $\gamma_h = \ln(\mu_3/\mu_1)$ on a crack inclined at 30 degrees such that the center of the crack is always kept in the middle of the interface. The distances a and b from the crack tips are the same from the lower and upper half plane, respectively.

Figures 3 and 4 show mode I and II of the normalized SIF at crack tip a versus the non-homogeneity constant $\ln(\mu_3/\mu_1)$. Observe that as $\ln(\mu_3/\mu_1)$ increases, both k_1 and k_2 decrease. The strongest effect is observed for the smallest thickness of the interface, while $h/c = 100$ may be considered as an infinite FGM plate, for which the SIF are virtually constant. When $\ln(\mu_3/\mu_1) = 0$, the plate is homogeneous, so the influence of the thickness of the interface disappears and the SIF become the same as for the infinite FGM plate.

Figures 5 and 6 represent mode I and II normalized SIF at crack tip b versus $\ln(\mu_3/\mu_1)$. The SIF curves increase with increasing $\ln(\mu_3/\mu_1)$, which is different from the behavior at tip a, except for the case of the infinite FGM plate. In addition to this behavior, the magnitude of the SIF tends to be higher at crack tip b than at tip a, especially for extreme values of $\ln(\mu_3/\mu_1)$.

Modes I and II of SERR are shown in Figure 7 and 8 for crack tip a and in Figure 9 and 10 for crack tip b. Notice that at both tips, SERR are decreasing with increasing stiffness of the upper half plane. Specifically, SERR at crack tip b behaves differently from the SIF at this tip. The behavior of SERR is more physically intuitive than the

unexpected behavior of the SIF. It should be recalled that the SERR is calculated using SIF and local material properties, so it contains more information than the SIF. For this reason the remaining parametric studies are discussed using only SERR data.

The influence of the orientation angle θ on the relation between SERR and the non-homogeneity constant at crack tip a for the case of the interface thickness $h/c=2$ under uniform shear stress at infinity is shown in Figures 11 and 12. As expected, the highest mode-I SERR is obtained for the smallest angle because of the high normal traction component acting on the surface of the crack. It can also be expected that the highest magnitude mode-II SERR is produced for $\theta=45$ degrees, since the shear traction component is maximized then. The behavior of the SERR at crack tip b is similar to the behavior at crack tip a, as can be deduced by comparison of Figures 7 and 9, and of 8 and 10. Hence, the magnitudes of the mode-I SERR at crack tip b are higher than at crack tip a, while the magnitudes of the mode-II SERR are smaller at crack tip b. In fact, the total SERR at crack tip b is equal to the total SERR at crack tip a.

In the next study, assume that the crack orientation is 30 degrees from the horizontal, and the thickness of the interface is $h=1$. Crack tip a is fixed at the distance $a/h = 0.1$ from the origin while crack tip b is at distance equal to $b/h= 0.3, 0.7$ and 1.1 along the x_1 axis, making the half of the crack length $c/h = 0.1, 0.3$ and 0.5 , respectively. Modes I and II normalized SERR at crack tip b are shown in Figures 13 and 14, respectively. Notice that the crack length significantly changes both SERR modes in the case of negative non-homogeneity constant. For the case where the upper half plane is stiffer than the lower half plane, the longer crack produces smaller normalized SERR.

Finally, assume constant crack length, constant orientation at 30 degrees and constant thickness of the interface FGM $h/c = 2$, and examine the influence of the position of the crack along the x_1 axis. Figures 15 and 16 show modes I and II normalized SERR at crack tip a versus the non-homogeneity constant for the crack defined by tip positions varying from 0.2 to 1.6 from the origin. Notice that the largest modes I and II SERR are obtained when $a/c = 1.6$ for negative non-homogeneity constant and when $a/c = 0.2$ for positive $\ln(\mu_3/\mu_1)$. Hence, the closer the crack tip is embedded to the stiffer material, the smaller the normalized SERR.

5. Conclusions

The analysis of an arbitrarily oriented crack in a strip of FGM sandwiched between two isotropic homogeneous half planes is done using singular integral equations. The equations are solved using Lobatto-Chebyshev integration, and give accurate results for mix-mode SIF and SERR.

Parametric studies show that SERR contain relevant information that is missing in the SIF, and therefore it is recommended that SERR be used as a driving force parameter for fracture problems of a crack in FGM. The model has shown that SERR are sensitive to the ratio of the shear moduli used as non-homogeneity constant. They are also sensitive to the ratio of thickness to the crack length. The longer the crack or the thinner the interface, the larger the SERR produced for negative values of $\ln(\mu_3/\mu_1)$, and the smaller the SERR produced for positive values of $\ln(\mu_3/\mu_1)$.

The crack orientation influence shows that SERR is proportional to the traction forces at the crack surface assumed in the perturbation problem. As the lower half plane becomes stiffer ($\ln(\mu_3/\mu_1)$ becomes more negative), both modes of the SERR become larger for every crack orientation. Clearly, the proper selection of the FGM parameters can reduce the driving forces of a crack embedded in the interface material.

References

- Asish Ghosh, Yoshinari Miyamoto, Ivar Reimanis and John J. Lannutti (eds.) (1997) "Functionally Graded Materials." Ceramic Trans., vol. 76.
- Binienda, W. K., and Arnold, S. M. (1995) "Driving Force Analysis in an Infinite Anisotropic Plate with Multiple Crack Interactions." International Journal of Fracture, Vol. 71, pp. 213-245.
- Chen, Y. F., Erdogan, F. (1996) "The Interface Crack Problem for a Non-Homogeneous Coatings Bonded to a Homogeneous Substrate." J. March. Phys. Solids, Vol. 44, No. 5, pp. 771-787, May.
- Delale, F., Erdogan, F. (1983) "The Crack Problem for a Non-Homogeneous Plan." Journal of Applied Mechanics, September, Vol. 50, pp. 609-614.
- Delale, F. and Erdogan, F. (1988) "On the Mechanical Modeling of the Interfacial Region in Bonded Half-Planes." Journal of Applied Mechanics, Vol. 55, June, pp. 317-324.
- Delale, F., Erdogan, F. (1988) "Interface Crack in a Non-Homogeneous Elastic Medium." Int. J., Engng Sci., Vol. 26, No. 6, pp. 559-568.
- Hirano, T., Yamada, T., Teraki, J., Niino, M. and Kumakawa, A. (1988). "A Study on Functionally Gradient Material Design System for a Thrust Chamber. Proc. 16th Int. Symp. On Space Technology and Science, Sapporo, Japan, May.
- Hirano, T. and Yamada, T. (1988). "Multi-Paradigm Expert System Architecture Based Upon the Inverse Design Concept." Int. Workshop on Artificial Intelligence for Industrial Applications, Hitachi, Japan, May 25-27.
- Holt J. Birch, Mitsue Koizumi, Toshio Hirai and Zuhir A. Munir (eds.) (1993) "Functionally Graded Materials." Ceramic Trans., vol. 34, The American Ceramic Society, Westerville, Ohio.
- Kawasaki, A. and Watanabe, R. (1990). "Fabrication of Sintered Functionally Gradient Material by Powder Spray Forming Process. FGM-90, proc. Of the 1st Int. symp. On FGM from, Sendai, Japan.
- Konda, N. and Erdogan, F. (1994) "The Mixed Mode Crack Problem in a Non-Homogeneous Elastic medium." Engineering Fracture Mechanics, Vol. 47, No. 4, pp. 533-545.
- Muskhelishvili, N. I., 1953, Singular Integral Equations. Noordhoff, Gronigen the Netherlands.
- Niino, M. and Maeda, S. (1990) "Recent Development Status of Functionally Gradient Materials." I. S. I. J. Int. 30, pp. 699-703.
- Shbeeb N. General Crack Problems in Functionally Graded Materials. Ph.D dissertation, 1998, The University of Akron.
- Tada, H. Patis, P. C. and Irwin G.R., 1985, "The Stress Analysis of Cracks Handbook", Del. Research Corp.
- Theocaris, P. S., and Ioakimidis, N. I., 1977, "Numerical Integration Methods for the Solution of Singular Integral Equations," Quarterly Of Appl. Math, pp. 173-183.

Table I Verification of the Solution.

γc	Konda and Erdogan (1994) $k_1(a)/\sqrt{c}$	Present Study $k_1(a)/\sqrt{c}$	Konda and Erdogan (1994) $k_2(a)/\sqrt{c}$	Present Study $k_2(a)/\sqrt{c}$
0.25	1.036	1.036	0.065	0.062
0.50	1.101	1.101	0.129	0.122
1.0	1.258	1.260	0.263	0.243

$c=(b-a)/2$

APPENDIX A

EXPRESSIONS OF THE CONSTANTS

It should be pointed out that all the algebraic manipulation were either verified or done by MATHEMATICA[®].

$$D_1 = A_1 + A_2 + A_3 + A_4 + g_1 B'_1 + g_2 B'_2$$

$$D_2 = (m_1 - |\alpha|)A_1 + (m_2 - |\alpha|)A_2 + (m_3 - |\alpha|)A_3 + (m_4 - |\alpha|)A_4 \\ - (|\alpha|g_1 - \frac{ig_3}{\alpha})B'_1 - (|\alpha|g_2 - \frac{ig_4}{\alpha})B'_2$$

$$C_1 = e^{|\alpha|h} [(1 - h(m_1 + |\alpha|))A_1 e^{m_1 h} + (1 - h(m_2 + |\alpha|))A_2 e^{m_2 h} \\ + (1 - h(m_3 + |\alpha|))A_3 e^{m_3 h} + (1 - h(m_4 + |\alpha|))A_4 e^{m_4 h} \\ + e^{i\alpha h \tan(\theta)} \{ (g_1(1 - h|\alpha|) - \frac{ihg_3}{\alpha})B'_1 e^{cn_1 h \sec(\theta)} + (g_2(1 - h|\alpha|) - \frac{ihg_4}{\alpha})B'_2 e^{cn_2 h \sec(\theta)} \}]$$

$$C_2 = e^{|\alpha|h} [(m_1 + |\alpha|)A_1 e^{m_1 h} + (m_2 + |\alpha|)A_2 e^{m_2 h} + (m_3 + |\alpha|)A_3 e^{m_3 h} \\ + (m_4 + |\alpha|)A_4 e^{m_4 h} + e^{i\alpha h \tan(\theta)} \{ (|\alpha|g_1 + \frac{ig_3}{\alpha})B'_1 e^{cn_1 h \sec(\theta)} \\ + (|\alpha|g_2 + \frac{ig_4}{\alpha})B'_2 e^{cn_2 h \sec(\theta)} \}]$$

$$g_1 = -\frac{\cos(\theta)}{\alpha^2} (cn_1 - i\alpha \cos(\theta))^2$$

$$g_2 = -\frac{\cos(\theta)}{\alpha^2} (cn_2 - i\alpha \cos(\theta))^2$$

$$g_3 = \cos(\theta)^2 (\alpha \sin(\theta) - i cn_1)(\alpha \cos(\theta) + i cn_1 \sin(\theta))$$

$$g_4 = \cos(\theta)^2 (\alpha \sin(\theta) - i cn_2)(\alpha \cos(\theta) + i cn_2 \sin(\theta))$$

$$\begin{aligned}
cn_1 &= \frac{1}{2} \left(\delta + \beta \sqrt{\frac{3 - \kappa_2}{\kappa_2 + 1}} \right) - \frac{1}{2} \sqrt{\left(\delta + \beta \sqrt{\frac{3 - \kappa_2}{\kappa_2 + 1}} \right)^2 + 4((\alpha \cos(\theta))^2 + i\alpha \cos(\theta) \left(\beta - \delta \sqrt{\frac{3 - \kappa_2}{\kappa_2 + 1}} \right))} \\
cn_2 &= \frac{1}{2} \left(\delta - \beta \sqrt{\frac{3 - \kappa_2}{\kappa_2 + 1}} \right) - \frac{1}{2} \sqrt{\left(\delta - \beta \sqrt{\frac{3 - \kappa_2}{\kappa_2 + 1}} \right)^2 + 4((\alpha \cos(\theta))^2 + i\alpha \cos(\theta) \left(\beta + \delta \sqrt{\frac{3 - \kappa_2}{\kappa_2 + 1}} \right))} \\
cn_3 &= \frac{1}{2} \left(\delta + \beta \sqrt{\frac{3 - \kappa_2}{\kappa_2 + 1}} \right) + \frac{1}{2} \sqrt{\left(\delta + \beta \sqrt{\frac{3 - \kappa_2}{\kappa_2 + 1}} \right)^2 + 4((\alpha \cos(\theta))^2 + i\alpha \cos(\theta) \left(\beta - \delta \sqrt{\frac{3 - \kappa_2}{\kappa_2 + 1}} \right))} \\
cn_4 &= \frac{1}{2} \left(\delta - \beta \sqrt{\frac{3 - \kappa_2}{\kappa_2 + 1}} \right) + \frac{1}{2} \sqrt{\left(\delta - \beta \sqrt{\frac{3 - \kappa_2}{\kappa_2 + 1}} \right)^2 + 4((\alpha \cos(\theta))^2 + i\alpha \cos(\theta) \left(\beta + \delta \sqrt{\frac{3 - \kappa_2}{\kappa_2 + 1}} \right))}
\end{aligned}$$

$$B'_1 = \frac{F_1(\alpha \cos(\theta))ch_{22} - F_2(\alpha \cos(\theta))ch_{12}}{ch_{11}ch_{22} - ch_{21}ch_{12}}$$

$$B'_2 = \frac{-F_1(\alpha \cos(\theta))ch_{21} + F_2(\alpha \cos(\theta))ch_{11}}{ch_{11}ch_{22} - ch_{21}ch_{12}}$$

$$ch_{11} = \frac{\kappa_2 + 1}{8\mu_0} (cn_1 - cn_3)(cn_1 - cn_4)$$

$$ch_{12} = \frac{\kappa_2 + 1}{8\mu_0} (cn_2 - cn_3)(cn_2 - cn_4)$$

$$ch_{21} = \frac{i\alpha \cos(\theta) - \beta}{8\mu_0} ((\alpha \cos(\theta))^2 (1 + \kappa_2) - \delta^2 (\kappa_2 - 3)) \left[\frac{(cn_1 - cn_3)(cn_1 - cn_4)}{(\delta - cn_1)(\delta - cn_3)(\delta - cn_4)} \right]$$

$$ch_{22} = \frac{i\alpha \cos(\theta) - \beta}{8\mu_0} ((\alpha \cos(\theta))^2 (1 + \kappa_2) - \delta^2 (\kappa_2 - 3)) \left[\frac{(cn_2 - cn_3)(cn_2 - cn_4)}{(\delta - cn_2)(\delta - cn_3)(\delta - cn_4)} \right]$$

$$\begin{aligned}
C_{11} &= 2 \frac{|\alpha|}{\alpha} m_1(\kappa_1 + 1) + \alpha(\kappa_2 - 2\kappa_1 - 1) - \frac{m_1^2(\kappa_2 + 1)}{\alpha} \\
C_{12} &= 2 \frac{|\alpha|}{\alpha} m_2(\kappa_1 + 1) + \alpha(\kappa_2 - 2\kappa_1 - 1) - \frac{m_2^2(\kappa_2 + 1)}{\alpha} \\
C_{13} &= 2 \frac{|\alpha|}{\alpha} m_3(\kappa_1 + 1) + \alpha(\kappa_2 - 2\kappa_1 - 1) - \frac{m_3^2(\kappa_2 + 1)}{\alpha} \\
C_{14} &= 2 \frac{|\alpha|}{\alpha} m_4(\kappa_1 + 1) + \alpha(\kappa_2 - 2\kappa_1 - 1) - \frac{m_4^2(\kappa_2 + 1)}{\alpha} \\
C_{21} &= 2m_1(\kappa_1 - 1) - 2|\alpha|(\kappa_1 + 1) - \frac{(\kappa_2 - 3)m_1^2 - \alpha^2(\kappa_2 + 1)}{m_1 - \gamma} \\
C_{22} &= 2m_2(\kappa_1 - 1) - 2|\alpha|(\kappa_1 + 1) - \frac{(\kappa_2 - 3)m_2^2 - \alpha^2(\kappa_2 + 1)}{m_2 - \gamma} \\
C_{23} &= 2m_3(\kappa_1 - 1) - 2|\alpha|(\kappa_1 + 1) - \frac{(\kappa_2 - 3)m_3^2 - \alpha^2(\kappa_2 + 1)}{m_3 - \gamma} \\
C_{24} &= 2m_4(\kappa_1 - 1) - 2|\alpha|(\kappa_1 + 1) - \frac{(\kappa_2 - 3)m_4^2 - \alpha^2(\kappa_2 + 1)}{m_4 - \gamma} \\
C_{31} &= [(2\alpha(1 - \kappa_3) - 2 \frac{|\alpha|}{\alpha} m_1(1 + \kappa_3)) + \alpha(\kappa_2 - 3) - \frac{m_1^2(\kappa_2 + 1)}{\alpha}] e^{m_1 h} \\
C_{32} &= [(2\alpha(1 - \kappa_3) - 2 \frac{|\alpha|}{\alpha} m_2(1 + \kappa_3)) + \alpha(\kappa_2 - 3) - \frac{m_2^2(\kappa_2 + 1)}{\alpha}] e^{m_2 h} \\
C_{33} &= [(2\alpha(1 - \kappa_3) - 2 \frac{|\alpha|}{\alpha} m_3(1 + \kappa_3)) + \alpha(\kappa_2 - 3) - \frac{m_3^2(\kappa_2 + 1)}{\alpha}] e^{m_3 h} \\
C_{34} &= [(2\alpha(1 - \kappa_3) - 2 \frac{|\alpha|}{\alpha} m_4(1 + \kappa_3)) + \alpha(\kappa_2 - 3) - \frac{m_4^2(\kappa_2 + 1)}{\alpha}] e^{m_4 h} \\
C_{41} &= [(4|\alpha| + 2(\kappa_3 - 1)(m_1 + |\alpha|)) - \frac{(\kappa_2 - 1)m_1^2 - \alpha^2(\kappa_2 + 1)}{m_1 - \gamma}] e^{m_1 h} \\
C_{42} &= [(4|\alpha| + 2(\kappa_3 - 1)(m_2 + |\alpha|)) - \frac{(\kappa_2 - 1)m_2^2 - \alpha^2(\kappa_2 + 1)}{m_2 - \gamma}] e^{m_2 h} \\
C_{43} &= [(4|\alpha| + 2(\kappa_3 - 1)(m_3 + |\alpha|)) - \frac{(\kappa_2 - 1)m_3^2 - \alpha^2(\kappa_2 + 1)}{m_3 - \gamma}] e^{m_3 h} \\
C_{44} &= [(4|\alpha| + 2(\kappa_3 - 1)(m_4 + |\alpha|)) - \frac{(\kappa_2 - 1)m_4^2 - \alpha^2(\kappa_2 + 1)}{m_4 - \gamma}] e^{m_4 h}
\end{aligned}$$

$$\begin{aligned}
J_1 &= S_1 \int_a^b f_1(t) e^{\beta t} e^{-i\alpha \cos(\theta)} dt + R_1 \int_a^b f_2(t) e^{\beta t} e^{-i\alpha \cos(\theta)} dt \\
S_1 &= \frac{g_6 ch_{21} - g_5 ch_{22}}{ch_{11} ch_{22} - ch_{12} ch_{21}} + \frac{2\alpha(1 - \kappa_1)(g_2 ch_{21} - g_1 ch_{22})}{ch_{11} ch_{22} - ch_{12} ch_{21}} + \frac{2i(\kappa_1 + 1)(g_4 ch_{21} - g_3 ch_{22})}{|\alpha|(ch_{11} ch_{22} - ch_{12} ch_{21})} \\
R_1 &= \frac{g_5 ch_{12} - g_6 ch_{11}}{ch_{11} ch_{22} - ch_{12} ch_{21}} + \frac{2\alpha(1 - \kappa_1)(g_1 ch_{12} - g_2 ch_{11})}{ch_{11} ch_{22} - ch_{12} ch_{21}} + \frac{2i(\kappa_1 + 1)(g_3 ch_{12} - g_4 ch_{11})}{|\alpha|(ch_{11} ch_{22} - ch_{12} ch_{21})} \\
J_2 &= S_2 \int_a^b f_1(t) e^{\beta t} e^{-i\alpha \cos(\theta)} dt + R_2 \int_a^b f_2(t) e^{\beta t} e^{-i\alpha \cos(\theta)} dt \\
S_2 &= \frac{g_7 ch_{22} - g_8 ch_{21}}{ch_{11} ch_{22} - ch_{12} ch_{21}} + \frac{2|\alpha|(1 + \kappa_1)(g_1 ch_{22} - g_2 ch_{21})}{ch_{11} ch_{22} - ch_{12} ch_{21}} + \frac{2i(\kappa_1 - 1)(g_4 ch_{21} - g_3 ch_{22})}{\alpha(ch_{11} ch_{22} - ch_{12} ch_{21})} \\
R_2 &= \frac{g_8 ch_{11} - g_7 ch_{12}}{ch_{11} ch_{22} - ch_{12} ch_{21}} + \frac{2|\alpha|(1 + \kappa_1)(g_2 ch_{11} - g_1 ch_{12})}{ch_{11} ch_{22} - ch_{12} ch_{21}} + \frac{2i(\kappa_1 - 1)(g_3 ch_{12} - g_4 ch_{11})}{\alpha(ch_{11} ch_{22} - ch_{12} ch_{21})} \\
J_3 &= S_3 \int_a^b f_1(t) e^{\beta t} e^{-i\alpha \cos(\theta)} dt + R_3 \int_a^b f_2(t) e^{\beta t} e^{-i\alpha \cos(\theta)} dt \\
S_3 &= e^{i\alpha h \tan(\theta)} \left[\frac{g_6 ch_{21} e^{cn_2 h \sec(\theta)} - g_5 ch_{22} e^{cn_1 h \sec(\theta)}}{ch_{11} ch_{22} - ch_{12} ch_{21}} - \frac{\mu_1 e^{\gamma h}}{\mu_3} \left(\frac{2\alpha(1 - \kappa_3)(g_1 ch_{22} e^{cn_1 h \sec(\theta)} - g_2 ch_{21} e^{cn_2 h \sec(\theta)})}{ch_{11} ch_{22} - ch_{12} ch_{21}} \right. \right. \\
&\quad \left. \left. + \frac{2i(\kappa_3 + 1)(g_4 ch_{21} e^{cn_2 h \sec(\theta)} - g_3 ch_{22} e^{cn_1 h \sec(\theta)})}{|\alpha|(ch_{11} ch_{22} - ch_{12} ch_{21})} \right) \right] \\
R_3 &= e^{i\alpha h \tan(\theta)} \left[\frac{g_5 ch_{12} e^{cn_1 h \sec(\theta)} - g_6 ch_{11} e^{cn_2 h \sec(\theta)}}{ch_{11} ch_{22} - ch_{12} ch_{21}} - \frac{\mu_1 e^{\gamma h}}{\mu_3} \left(\frac{2\alpha(1 - \kappa_3)(g_2 ch_{11} e^{cn_2 h \sec(\theta)} - g_1 ch_{12} e^{cn_1 h \sec(\theta)})}{ch_{11} ch_{22} - ch_{12} ch_{21}} \right. \right. \\
&\quad \left. \left. + \frac{2i(\kappa_3 + 1)(g_3 ch_{12} e^{cn_1 h \sec(\theta)} - g_4 ch_{11} e^{cn_2 h \sec(\theta)})}{|\alpha|(ch_{11} ch_{22} - ch_{12} ch_{21})} \right) \right] \\
J_4 &= S_4 \int_a^b f_1(t) e^{\beta t} e^{-i\alpha \cos(\theta)} dt + R_4 \int_a^b f_2(t) e^{\beta t} e^{-i\alpha \cos(\theta)} dt \\
S_4 &= e^{i\alpha h \tan(\theta)} \left[\frac{g_7 ch_{22} e^{cn_1 h \sec(\theta)} - g_8 ch_{21} e^{cn_2 h \sec(\theta)}}{ch_{11} ch_{22} - ch_{12} ch_{21}} - \frac{\mu_1 e^{\gamma h}}{\mu_3} \left(\frac{2|\alpha|(1 + \kappa_3)(g_1 ch_{22} e^{cn_1 h \sec(\theta)} - g_2 ch_{21} e^{cn_2 h \sec(\theta)})}{ch_{11} ch_{22} - ch_{12} ch_{21}} \right. \right. \\
&\quad \left. \left. + \frac{2i(\kappa_3 - 1)(g_3 ch_{22} e^{cn_1 h \sec(\theta)} - g_4 ch_{21} e^{cn_2 h \sec(\theta)})}{\alpha(ch_{11} ch_{22} - ch_{12} ch_{21})} \right) \right] \\
R_4 &= e^{i\alpha h \tan(\theta)} \left[\frac{g_8 ch_{11} e^{cn_2 h \sec(\theta)} - g_7 ch_{12} e^{cn_1 h \sec(\theta)}}{ch_{11} ch_{22} - ch_{12} ch_{21}} - \frac{\mu_1 e^{\gamma h}}{\mu_3} \left(\frac{2|\alpha|(1 + \kappa_3)(g_2 ch_{11} e^{cn_2 h \sec(\theta)} - g_1 ch_{12} e^{cn_1 h \sec(\theta)})}{ch_{11} ch_{22} - ch_{12} ch_{21}} \right. \right. \\
&\quad \left. \left. + \frac{2i(\kappa_3 - 1)(g_4 ch_{11} e^{cn_2 h \sec(\theta)} - g_3 ch_{12} e^{cn_1 h \sec(\theta)})}{\alpha(ch_{11} ch_{22} - ch_{12} ch_{21})} \right) \right]
\end{aligned}$$

$$\begin{aligned}
g_5 &= \cos(\theta) \left[\frac{\alpha^2 \cos(\theta)^2 (\kappa_2 - 3) - cn_1^2 (\kappa_2 + 1)}{\alpha \cos(\theta) + i\beta} \cos(\theta) - \frac{\alpha^2 \cos(\theta)^2 (\kappa_2 + 1) - cn_1^2 (\kappa_2 - 3)}{i(\delta - cn_1)} \sin(\theta) \right] \\
g_6 &= \cos(\theta) \left[\frac{\alpha^2 \cos(\theta)^2 (\kappa_2 - 3) - cn_2^2 (\kappa_2 + 1)}{\alpha \cos(\theta) + i\beta} \cos(\theta) - \frac{\alpha^2 \cos(\theta)^2 (\kappa_2 + 1) - cn_2^2 (\kappa_2 - 3)}{i(\delta - cn_2)} \sin(\theta) \right] \\
g_7 &= \cos(\theta) \left[\frac{\alpha^2 \cos(\theta)^2 (\kappa_2 + 1) - cn_1^2 (\kappa_2 - 3)}{\delta - cn_1} \cos(\theta) + i \frac{\alpha^2 \cos(\theta)^2 (\kappa_2 - 3) - cn_1^2 (\kappa_2 + 1)}{\alpha \cos(\theta) + i\beta} \sin(\theta) \right] \\
g_8 &= \cos(\theta) \left[\frac{\alpha^2 \cos(\theta)^2 (\kappa_2 + 1) - cn_2^2 (\kappa_2 - 3)}{\delta - cn_2} \cos(\theta) + i \frac{\alpha^2 \cos(\theta)^2 (\kappa_2 - 3) - cn_2^2 (\kappa_2 + 1)}{\alpha \cos(\theta) + i\beta} \sin(\theta) \right]
\end{aligned}$$

$$\begin{aligned}
Y_{11} &= (i\alpha \cos(\theta) + m_1 \sin(\theta))^2 \left(\frac{Q_{11}}{Q} S_1 - \frac{Q_{12}}{Q} S_2 + \frac{Q_{13}}{Q} S_3 - \frac{Q_{14}}{Q} S_4 \right) e^{m_1 x_1 \sin(\theta)} \\
&\quad + (i\alpha \cos(\theta) + m_2 \sin(\theta))^2 \left(-\frac{Q_{21}}{Q} S_1 + \frac{Q_{22}}{Q} S_2 - \frac{Q_{23}}{Q} S_3 + \frac{Q_{24}}{Q} S_4 \right) e^{m_2 x_1 \sin(\theta)} \\
&\quad + (i\alpha \cos(\theta) + m_3 \sin(\theta))^2 \left(\frac{Q_{31}}{Q} S_1 - \frac{Q_{32}}{Q} S_2 + \frac{Q_{33}}{Q} S_3 - \frac{Q_{34}}{Q} S_4 \right) e^{m_3 x_1 \sin(\theta)} \\
&\quad + (i\alpha \cos(\theta) + m_4 \sin(\theta))^2 \left(-\frac{Q_{41}}{Q} S_1 + \frac{Q_{42}}{Q} S_2 - \frac{Q_{43}}{Q} S_3 + \frac{Q_{44}}{Q} S_4 \right) e^{m_4 x_1 \sin(\theta)} \\
Y_{12} &= (i\alpha \cos(\theta) + m_1 \sin(\theta))^2 \left(\frac{Q_{11}}{Q} R_1 - \frac{Q_{12}}{Q} R_2 + \frac{Q_{13}}{Q} R_3 - \frac{Q_{14}}{Q} R_4 \right) e^{m_1 x_1 \sin(\theta)} \\
&\quad + (i\alpha \cos(\theta) + m_2 \sin(\theta))^2 \left(-\frac{Q_{21}}{Q} R_1 + \frac{Q_{22}}{Q} R_2 - \frac{Q_{23}}{Q} R_3 + \frac{Q_{24}}{Q} R_4 \right) e^{m_2 x_1 \sin(\theta)} \\
&\quad + (i\alpha \cos(\theta) + m_3 \sin(\theta))^2 \left(\frac{Q_{31}}{Q} R_1 - \frac{Q_{32}}{Q} R_2 + \frac{Q_{33}}{Q} R_3 - \frac{Q_{34}}{Q} R_4 \right) e^{m_3 x_1 \sin(\theta)} \\
&\quad + (i\alpha \cos(\theta) + m_4 \sin(\theta))^2 \left(-\frac{Q_{41}}{Q} R_1 + \frac{Q_{42}}{Q} R_2 - \frac{Q_{43}}{Q} R_3 + \frac{Q_{44}}{Q} R_4 \right) e^{m_4 x_1 \sin(\theta)}
\end{aligned}$$

$$\begin{aligned}
Y_{21} = & (\sin(\theta)\cos(\theta)(m_1^2 + \alpha^2) + im_1\alpha(\cos(\theta)^2 - \sin(\theta)^2))\left(\frac{Q_{11}}{Q}S_1 - \frac{Q_{12}}{Q}S_2 + \frac{Q_{13}}{Q}S_3\right. \\
& \left. - \frac{Q_{14}}{Q}S_4\right)e^{m_1x_1\sin(\theta)} \\
& + (\sin(\theta)\cos(\theta)(m_2^2 + \alpha^2) + im_2\alpha(\cos(\theta)^2 - \sin(\theta)^2))\left(-\frac{Q_{21}}{Q}S_1 + \frac{Q_{22}}{Q}S_2 - \frac{Q_{23}}{Q}S_3\right. \\
& \left. + \frac{Q_{24}}{Q}S_4\right)e^{m_2x_1\sin(\theta)} \\
& + (\sin(\theta)\cos(\theta)(m_3^2 + \alpha^2) + im_3\alpha(\cos(\theta)^2 - \sin(\theta)^2))\left(\frac{Q_{31}}{Q}S_1 - \frac{Q_{32}}{Q}S_2 + \frac{Q_{33}}{Q}S_3\right. \\
& \left. - \frac{Q_{34}}{Q}S_4\right)e^{m_3x_1\sin(\theta)} \\
& + (\sin(\theta)\cos(\theta)(m_4^2 + \alpha^2) + im_4\alpha(\cos(\theta)^2 - \sin(\theta)^2))\left(-\frac{Q_{41}}{Q}S_1 + \frac{Q_{42}}{Q}S_2 - \frac{Q_{43}}{Q}S_3\right. \\
& \left. + \frac{Q_{44}}{Q}S_4\right)e^{m_4x_1\sin(\theta)}
\end{aligned}$$

$$\begin{aligned}
Y_{22} = & (\sin(\theta)\cos(\theta)(m_1^2 + \alpha^2) + im_1\alpha(\cos(\theta)^2 - \sin(\theta)^2))\left(\frac{Q_{11}}{Q}R_1 - \frac{Q_{12}}{Q}R_2 + \frac{Q_{13}}{Q}R_3\right. \\
& \left. - \frac{Q_{14}}{Q}R_4\right)e^{m_1x_1\sin(\theta)} \\
& + (\sin(\theta)\cos(\theta)(m_2^2 + \alpha^2) + im_2\alpha(\cos(\theta)^2 - \sin(\theta)^2))\left(-\frac{Q_{21}}{Q}R_1 + \frac{Q_{22}}{Q}R_2 - \frac{Q_{23}}{Q}R_3\right. \\
& \left. + \frac{Q_{24}}{Q}R_4\right)e^{m_2x_1\sin(\theta)} \\
& + (\sin(\theta)\cos(\theta)(m_3^2 + \alpha^2) + im_3\alpha(\cos(\theta)^2 - \sin(\theta)^2))\left(\frac{Q_{31}}{Q}R_1 - \frac{Q_{32}}{Q}R_2 + \frac{Q_{33}}{Q}R_3\right. \\
& \left. - \frac{Q_{34}}{Q}R_4\right)e^{m_3x_1\sin(\theta)} \\
& + (\sin(\theta)\cos(\theta)(m_4^2 + \alpha^2) + im_4\alpha(\cos(\theta)^2 - \sin(\theta)^2))\left(-\frac{Q_{41}}{Q}R_1 + \frac{Q_{42}}{Q}R_2 - \frac{Q_{43}}{Q}R_3\right. \\
& \left. + \frac{Q_{44}}{Q}R_4\right)e^{m_4x_1\sin(\theta)}
\end{aligned}$$

APPENDIX B

$$a_{11} = \text{real}(l_{11}), c_{11} = \text{real}(\text{const11}), b_{11} = \text{imaginary}(l_{11}), d_{11} = \text{imaginary}(\text{const11})$$

$$a_{12} = \text{real}(l_{12}), c_{12} = \text{real}(\text{const12}), b_{12} = \text{imaginary}(l_{12}), d_{12} = \text{imaginary}(\text{const12})$$

$$a_{21} = -\text{real}(l_{21}), c_{21} = -\text{real}(\text{const21}), b_{21} = -\text{imaginary}(l_{21}), d_{21} = -\text{imaginary}(\text{const21})$$

$$a_{22} = -\text{real}(l_{22}), c_{22} = -\text{real}(\text{const22}), b_{22} = -\text{imaginary}(l_{22}), d_{22} = -\text{imaginary}(\text{const22})$$

where

$$l_{11} = - \frac{2 I E^{-\text{imag1}+2 I \theta} (-1 + E^{\text{imag1}}) (1 + E^{\text{imag1}}) \alpha \left(\frac{1}{1+\kappa_2} \right)^{3/2} (\text{Cos}[\theta] + E^{I \theta} \kappa_2)}{\gamma \sqrt{3 - \kappa_2}}$$

$$\text{const11} = E^{\text{imag1}} \left(\gamma (\text{Cos}[\theta] + I \text{Sin}[\theta]) \text{Sin}[\theta] \left(I + \sqrt{\frac{3 - \kappa_2}{1 + \kappa_2}} \right) \right.$$

$$\left(- \frac{\left(\frac{1}{1+\kappa_2} \right)^{3/2} (\text{Sin}[\theta] + (I \text{Cos}[3 \theta] + \text{Sin}[\theta] + \text{Sin}[3 \theta]) \kappa_1 + (-I \text{Cos}[\theta] + \text{Sin}[\theta]) \kappa_2)}{\gamma \sqrt{3 - \kappa_2}} + \right.$$

$$\left. \left. \frac{I \left(\frac{1}{1+\kappa_2} \right)^{3/2} (4 (\text{Cos}[3 \theta] - 4 I \text{Cos}[\theta]^2 \text{Sin}[\theta]) \kappa_1 + 4 I \text{Sin}[\theta] (-1 + \kappa_2) + 4 \text{Cos}[\theta] (2 + \kappa_2))}{4 \gamma \sqrt{3 - \kappa_2}} \right) - \right.$$

$$(\text{Cos}[\theta] + I \text{Sin}[\theta])^2 \left(\frac{1}{4 (1 + \kappa_1) (-3 + \kappa_2) (1 + \kappa_2)^2} \right.$$

$$\left(I (\text{Sin}[\theta] + (I \text{Cos}[3 \theta] + \text{Sin}[\theta] + \text{Sin}[3 \theta]) \kappa_1 + (-I \text{Cos}[\theta] + \text{Sin}[\theta]) \kappa_2) \right.$$

$$\left. \left(-6 - 3 \kappa_1 + \kappa_2 (-1 + \kappa_1 + \kappa_2) + I \sqrt{\frac{3 - \kappa_2}{1 + \kappa_2}} (-4 - 3 \kappa_1 - \kappa_2 - \kappa_1 \kappa_2 + \kappa_2^2) \right) \right) +$$

$$\frac{1}{16 (1 + \kappa_1) (-3 + \kappa_2) (1 + \kappa_2)^2}$$

$$\left((4 (\text{Cos}[3 \theta] - 4 I \text{Cos}[\theta]^2 \text{Sin}[\theta]) \kappa_1 + 4 I \text{Sin}[\theta] (-1 + \kappa_2) + 4 \text{Cos}[\theta] (2 + \kappa_2)) \right.$$

$$\left. \left(-3 \kappa_1 - \kappa_2 (-3 - \kappa_1 + \kappa_2) - I \sqrt{\frac{3 - \kappa_2}{1 + \kappa_2}} (2 + 3 \kappa_1 + \kappa_2 (1 + \kappa_1 + \kappa_2)) \right) \right) \right) +$$

$$\begin{aligned}
& \mathbf{E}^{\text{imag3}} \left(-\gamma (\text{Cos}[\theta] + \mathbf{I} \text{Sin}[\theta]) \text{Sin}[\theta] \left(-\mathbf{I} + \sqrt{\frac{3-\kappa_2}{1+\kappa_2}} \right) \right. \\
& \left. - \frac{\sqrt{\frac{3-\kappa_2}{1+\kappa_2}} (\text{Sin}[\theta] + (\mathbf{I} \text{Cos}[3\theta] + \text{Sin}[\theta] + \text{Sin}[3\theta]) \kappa_1 + (-\mathbf{I} \text{Cos}[\theta] + \text{Sin}[\theta]) \kappa_2)}{\gamma (-3 + \kappa_2) (1 + \kappa_2)} + \right. \\
& \left. \frac{\mathbf{I} \sqrt{\frac{3-\kappa_2}{1+\kappa_2}} (4 (\text{Cos}[3\theta] - 4 \mathbf{I} \text{Cos}[\theta]^2 \text{Sin}[\theta]) \kappa_1 + 4 \mathbf{I} \text{Sin}[\theta] (-1 + \kappa_2) + 4 \text{Cos}[\theta] (2 + \kappa_2))}{4 \gamma (-3 + \kappa_2) (1 + \kappa_2)} \right) - \\
& (\text{Cos}[\theta] + \mathbf{I} \text{Sin}[\theta])^2 \left(\frac{1}{4 (1 + \kappa_1) (-3 + \kappa_2) (1 + \kappa_2)^2} \right. \\
& \left(\mathbf{I} (\text{Sin}[\theta] + (\mathbf{I} \text{Cos}[3\theta] + \text{Sin}[\theta] + \text{Sin}[3\theta]) \kappa_1 + (-\mathbf{I} \text{Cos}[\theta] + \text{Sin}[\theta]) \kappa_2) \right. \\
& \left. \left(-6 - 3 \kappa_1 + \kappa_2 (-1 + \kappa_1 + \kappa_2) - \mathbf{I} \sqrt{\frac{3-\kappa_2}{1+\kappa_2}} (-4 - 3 \kappa_1 + \kappa_2 (-1 - \kappa_1 + \kappa_2)) \right) \right) + \\
& \frac{1}{16 (1 + \kappa_1) (-3 + \kappa_2) (1 + \kappa_2)^2} \\
& \left((4 (\text{Cos}[3\theta] - 4 \mathbf{I} \text{Cos}[\theta]^2 \text{Sin}[\theta]) \kappa_1 + 4 \mathbf{I} \text{Sin}[\theta] (-1 + \kappa_2) + 4 \text{Cos}[\theta] (2 + \kappa_2)) \right. \\
& \left. \left(-3 \kappa_1 - \kappa_2 (-3 - \kappa_1 + \kappa_2) + \mathbf{I} \sqrt{\frac{3-\kappa_2}{1+\kappa_2}} (2 + 3 \kappa_1 + \kappa_2 (1 + \kappa_1 + \kappa_2)) \right) \right) \Bigg) \\
\text{li2} = & \frac{2 \mathbf{E}^{-\text{imag1}+2\mathbf{I}\theta} (-1 + \mathbf{E}^{2\text{imag1}}) \alpha \left(\frac{1}{1+\kappa_2} \right)^{3/2} (\text{Cos}[\theta] + \mathbf{E}^{\mathbf{I}\theta} \kappa_2)}{\gamma \sqrt{3-\kappa_2}} \\
\text{const12} = & \mathbf{E}^{\text{imag1}} \left(\gamma (\text{Cos}[\theta] + \mathbf{I} \text{Sin}[\theta]) \text{Sin}[\theta] \left(\mathbf{I} + \sqrt{\frac{3-\kappa_2}{1+\kappa_2}} \right) \right. \\
& \left(-\frac{\mathbf{I} \left(\frac{1}{1+\kappa_2} \right)^{3/2} (-2 \mathbf{I} \text{Cos}[\theta] - \text{Sin}[\theta] - \mathbf{I} \text{Cos}[\theta] \kappa_1 - \mathbf{I} \text{Cos}[\theta] \kappa_2 + \text{Sin}[\theta] \kappa_2)}{\gamma \sqrt{3-\kappa_2}} - \right. \\
& \left. \left. \frac{\mathbf{I} \left(\frac{1}{1+\kappa_2} \right)^{3/2} (\text{Sin}[\theta] + \mathbf{I} \text{Cos}[\theta] \kappa_1 - \mathbf{I} \text{Cos}[\theta] \kappa_2 + \text{Sin}[\theta] \kappa_2)}{\gamma \sqrt{3-\kappa_2}} \right) \right) -
\end{aligned}$$

$$\begin{aligned}
& (\cos[\theta] + i \sin[\theta])^2 \\
& \left(-\frac{1}{4(1+\kappa_1)(-3+\kappa_2)(1+\kappa_2)^2} \left((-2i \cos[\theta] - \sin[\theta] - i \cos[\theta] \kappa_1 - i \cos[\theta] \kappa_2 + \sin[\theta] \kappa_2) \right. \right. \\
& \quad \left. \left(-6 - 3\kappa_1 + \kappa_2(-1 + \kappa_1 + \kappa_2) + i \sqrt{\frac{3-\kappa_2}{1+\kappa_2}} (-4 - 3\kappa_1 - \kappa_2 - \kappa_1 \kappa_2 + \kappa_2^2) \right) \right) - \\
& \quad \left((\sin[\theta] + i \cos[\theta] \kappa_1 - i \cos[\theta] \kappa_2 + \sin[\theta] \kappa_2) \right. \\
& \quad \left. \left(-3\kappa_1 - \kappa_2(-3 - \kappa_1 + \kappa_2) - i \sqrt{\frac{3-\kappa_2}{1+\kappa_2}} (2 + 3\kappa_1 + \kappa_2(1 + \kappa_1 + \kappa_2)) \right) \right) / \\
& \quad \left. (4(1+\kappa_1)(-3+\kappa_2)(1+\kappa_2)^2) \right) \Bigg) + \\
& \mathbf{E}^{\text{imag}^3} \left(-\gamma (\cos[\theta] + i \sin[\theta]) \sin[\theta] \left(-i + \sqrt{\frac{3-\kappa_2}{1+\kappa_2}} \right) \right. \\
& \quad \left(-\frac{i \sqrt{\frac{3-\kappa_2}{1+\kappa_2}} (-2i \cos[\theta] - \sin[\theta] - i \cos[\theta] \kappa_1 - i \cos[\theta] \kappa_2 + \sin[\theta] \kappa_2)}{\gamma(-3+\kappa_2)(1+\kappa_2)} - \right. \\
& \quad \left. \frac{i \sqrt{\frac{3-\kappa_2}{1+\kappa_2}} (\sin[\theta] + i \cos[\theta] \kappa_1 - i \cos[\theta] \kappa_2 + \sin[\theta] \kappa_2)}{\gamma(-3+\kappa_2)(1+\kappa_2)} \right) - \\
& (\cos[\theta] + i \sin[\theta])^2 \\
& \left(-\frac{1}{4(1+\kappa_1)(-3+\kappa_2)(1+\kappa_2)^2} \left((-2i \cos[\theta] - \sin[\theta] - i \cos[\theta] \kappa_1 - i \cos[\theta] \kappa_2 + \sin[\theta] \kappa_2) \right. \right. \\
& \quad \left. \left(-6 - 3\kappa_1 + \kappa_2(-1 + \kappa_1 + \kappa_2) - i \sqrt{\frac{3-\kappa_2}{1+\kappa_2}} (-4 - 3\kappa_1 + \kappa_2(-1 - \kappa_1 + \kappa_2)) \right) \right) - \\
& \quad \left((\sin[\theta] + i \cos[\theta] \kappa_1 - i \cos[\theta] \kappa_2 + \sin[\theta] \kappa_2) \right. \\
& \quad \left. \left(-3\kappa_1 - \kappa_2(-3 - \kappa_1 + \kappa_2) + i \sqrt{\frac{3-\kappa_2}{1+\kappa_2}} (2 + 3\kappa_1 + \kappa_2(1 + \kappa_1 + \kappa_2)) \right) \right) / \\
& \quad \left. (4(1+\kappa_1)(-3+\kappa_2)(1+\kappa_2)^2) \right) \Bigg)
\end{aligned}$$

$$\begin{aligned}
l21 &= \frac{2 E^{-\text{imag}1+2I\theta} (-1 + E^{2\text{imag}1}) \alpha \left(\frac{1}{1+\kappa_2} \right)^{3/2} (\text{Cos}[\theta] + E^{I\theta} \kappa_2)}{\gamma \sqrt{3-\kappa_2}} \\
\text{const21} &= E^{\text{imag}1} \left(\frac{1}{2} \gamma (\text{Cos}[\theta] + I \text{Sin}[\theta])^2 \left(I + \sqrt{\frac{3-\kappa_2}{1+\kappa_2}} \right) \right. \\
&\quad \left(-\frac{\left(\frac{1}{1+\kappa_2} \right)^{3/2} (\text{Sin}[\theta] + (I \text{Cos}[3\theta] + \text{Sin}[\theta] + \text{Sin}[3\theta]) \kappa_1 + (-I \text{Cos}[\theta] + \text{Sin}[\theta]) \kappa_2)}{\gamma \sqrt{3-\kappa_2}} + \frac{1}{4 \gamma \sqrt{3-\kappa_2}} \right. \\
&\quad \left. \left(I \left(\frac{1}{1+\kappa_2} \right)^{3/2} (4 (\text{Cos}[3\theta] - 4 I \text{Cos}[\theta]^2 \text{Sin}[\theta]) \kappa_1 + 4 I \text{Sin}[\theta] (-1 + \kappa_2) + 4 \text{Cos}[\theta] (2 + \kappa_2)) \right) \right) - \\
&\quad I (\text{Cos}[\theta] + I \text{Sin}[\theta])^2 \left(\frac{1}{4 (1 + \kappa_1) (-3 + \kappa_2) (1 + \kappa_2)^2} \right. \\
&\quad \left(I (\text{Sin}[\theta] + (I \text{Cos}[3\theta] + \text{Sin}[\theta] + \text{Sin}[3\theta]) \kappa_1 + (-I \text{Cos}[\theta] + \text{Sin}[\theta]) \kappa_2) \right. \\
&\quad \left. \left(-6 - 3 \kappa_1 + \kappa_2 (-1 + \kappa_1 + \kappa_2) + I \sqrt{\frac{3-\kappa_2}{1+\kappa_2}} (-4 - 3 \kappa_1 - \kappa_2 - \kappa_1 \kappa_2 + \kappa_2^2) \right) \right) + \\
&\quad \frac{1}{16 (1 + \kappa_1) (-3 + \kappa_2) (1 + \kappa_2)^2} \\
&\quad \left((4 (\text{Cos}[3\theta] - 4 I \text{Cos}[\theta]^2 \text{Sin}[\theta]) \kappa_1 + 4 I \text{Sin}[\theta] (-1 + \kappa_2) + 4 \text{Cos}[\theta] (2 + \kappa_2)) \right. \\
&\quad \left. \left(-3 \kappa_1 - \kappa_2 (-3 - \kappa_1 + \kappa_2) - I \sqrt{\frac{3-\kappa_2}{1+\kappa_2}} (2 + 3 \kappa_1 + \kappa_2 (1 + \kappa_1 + \kappa_2)) \right) \right) \right) + \\
&\quad E^{\text{imag}3} \left(-\frac{1}{2} \gamma (\text{Cos}[\theta] + I \text{Sin}[\theta])^2 \left(-I + \sqrt{\frac{3-\kappa_2}{1+\kappa_2}} \right) \right. \\
&\quad \left(-\frac{\sqrt{\frac{3-\kappa_2}{1+\kappa_2}} (\text{Sin}[\theta] + (I \text{Cos}[3\theta] + \text{Sin}[\theta] + \text{Sin}[3\theta]) \kappa_1 + (-I \text{Cos}[\theta] + \text{Sin}[\theta]) \kappa_2)}{\gamma (-3 + \kappa_2) (1 + \kappa_2)} + \right. \\
&\quad \left. \frac{I \sqrt{\frac{3-\kappa_2}{1+\kappa_2}} (4 (\text{Cos}[3\theta] - 4 I \text{Cos}[\theta]^2 \text{Sin}[\theta]) \kappa_1 + 4 I \text{Sin}[\theta] (-1 + \kappa_2) + 4 \text{Cos}[\theta] (2 + \kappa_2))}{4 \gamma (-3 + \kappa_2) (1 + \kappa_2)} \right) -
\end{aligned}$$

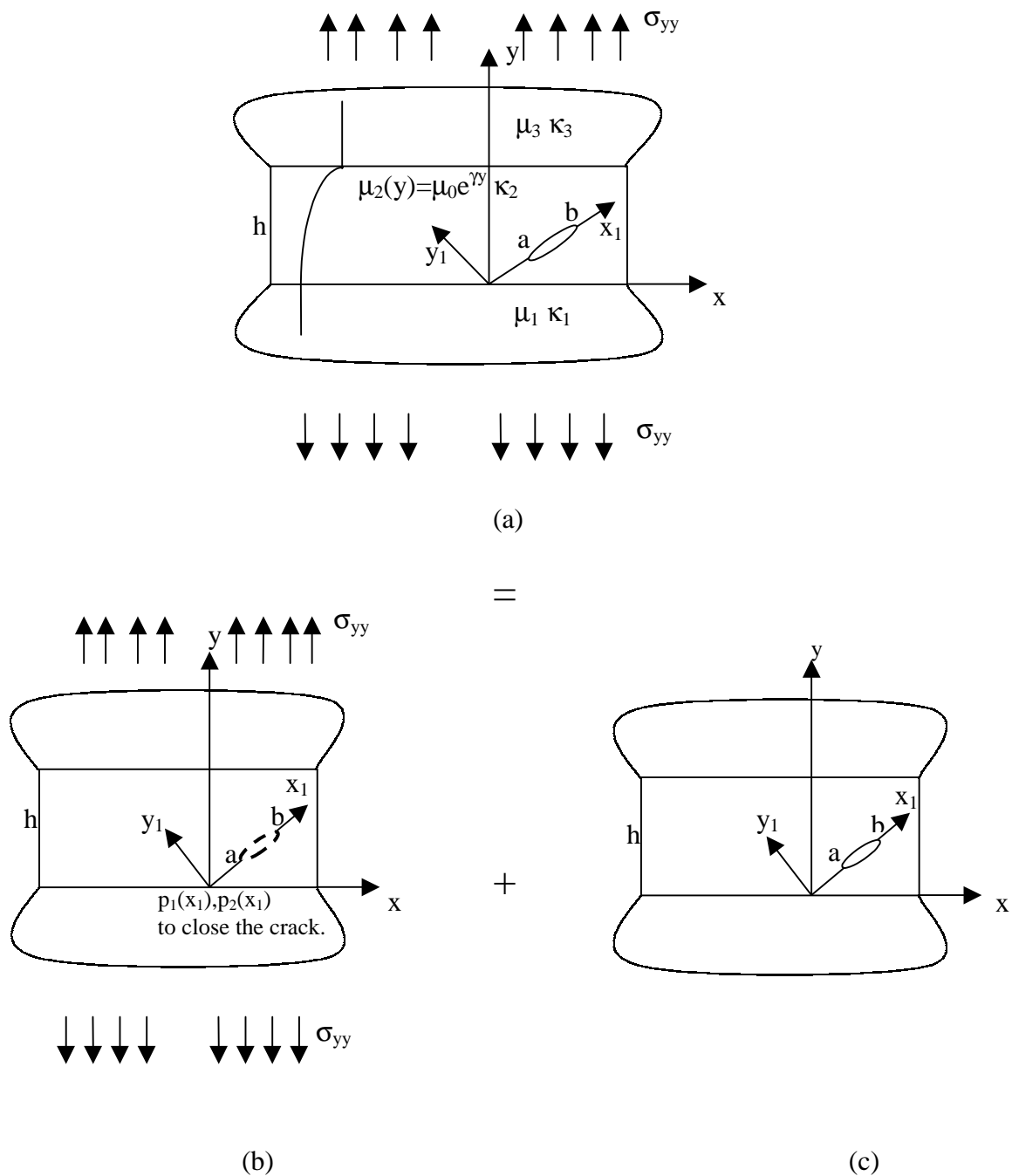


Figure 1. Formulation of the Perturbation Problem.
 (a). The Original Problem.
 (b). The Elasticity Problem.
 (c). The Mixed Boundary Value Problem.

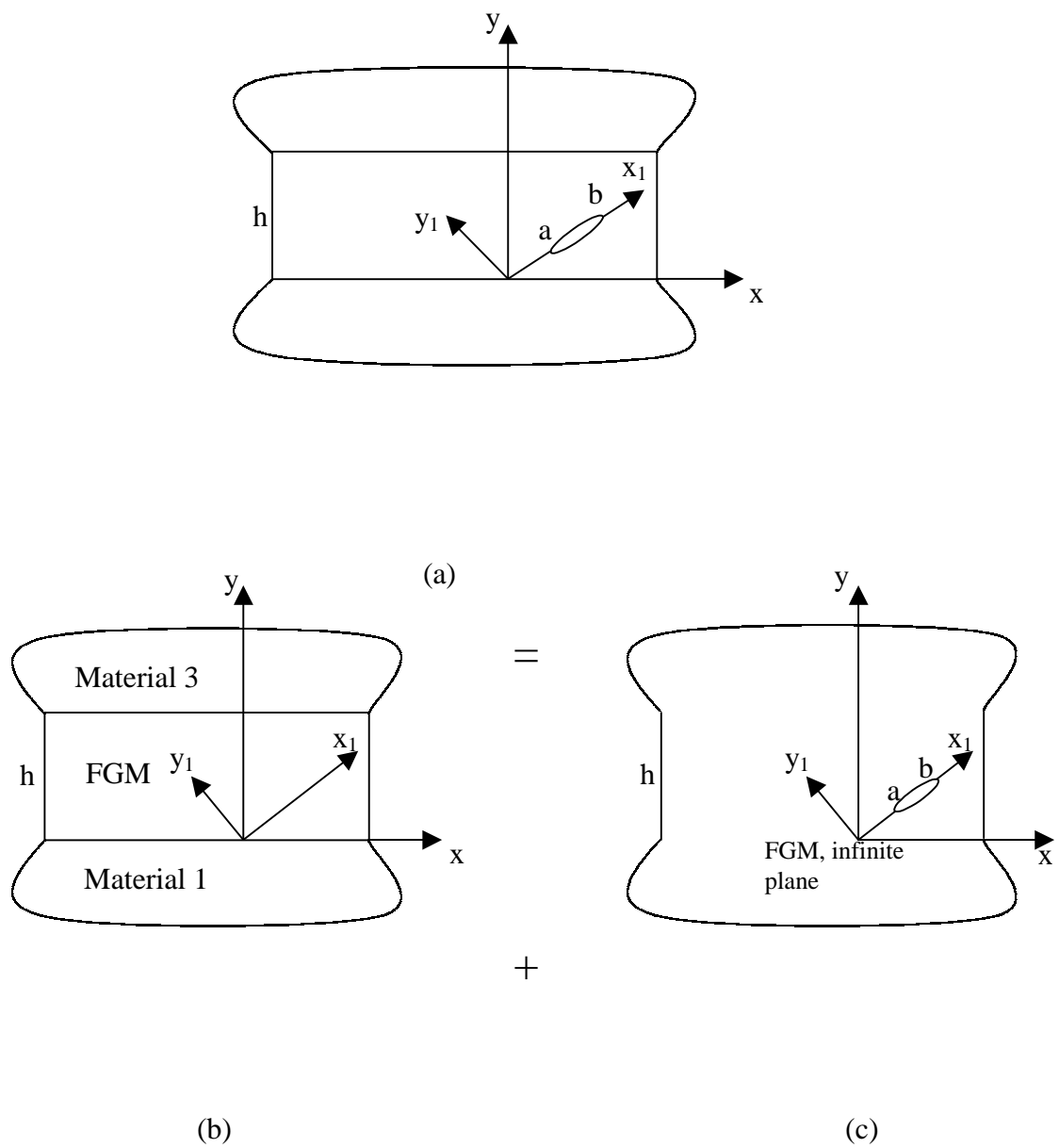


Figure 2. Methodology of the solution of the Perturbation Problem
 (a). The Mixed Boundary Value Problem
 (b). Infinite FGM Strip Without Crack
 (c). Infinite FGM Plate With Crack

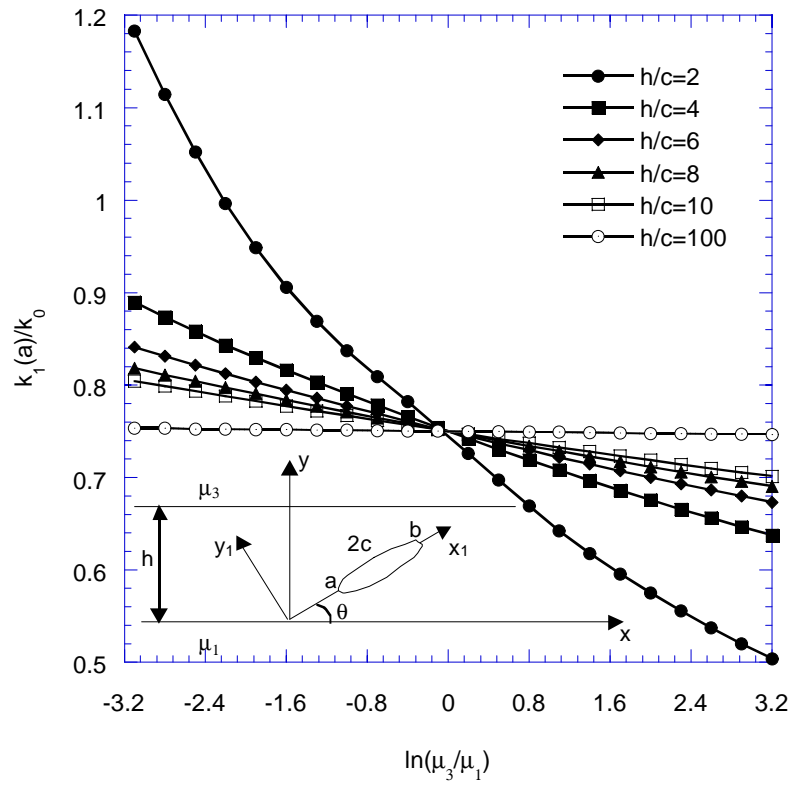


Figure 3. Normalized mode I SIF at crack tip (a) for various h/c , $\theta=30$ deg. and center of the crack is located at $h/2$, under loading of uniform normal stress.

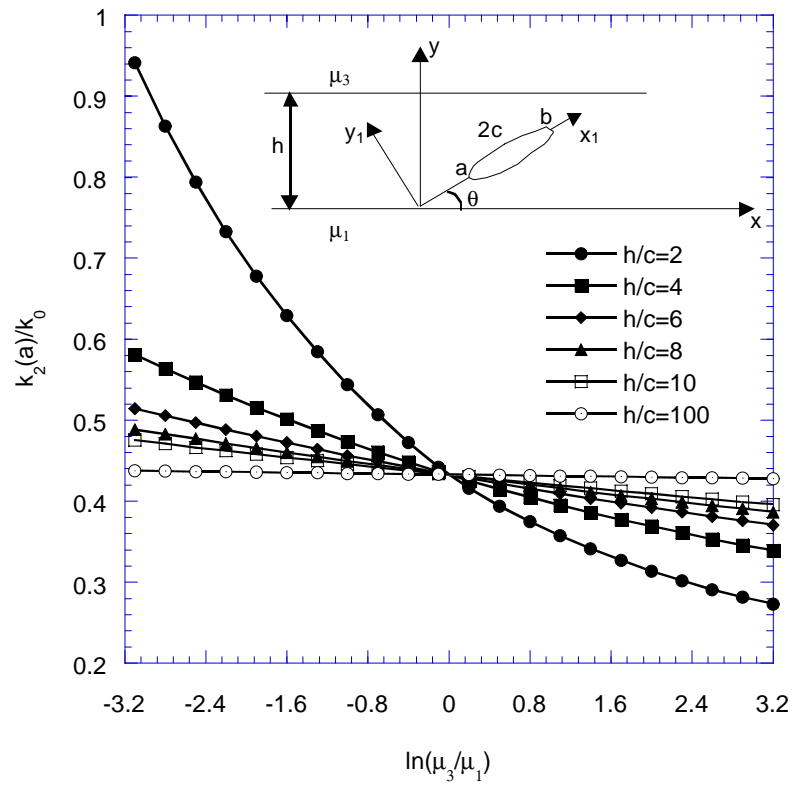


Figure 4. Normalized mode II SIF at crack tip (a) for various h/c , $\theta=30$ deg. and center of the crack is located at $h/2$, under loading of uniform normal stress.

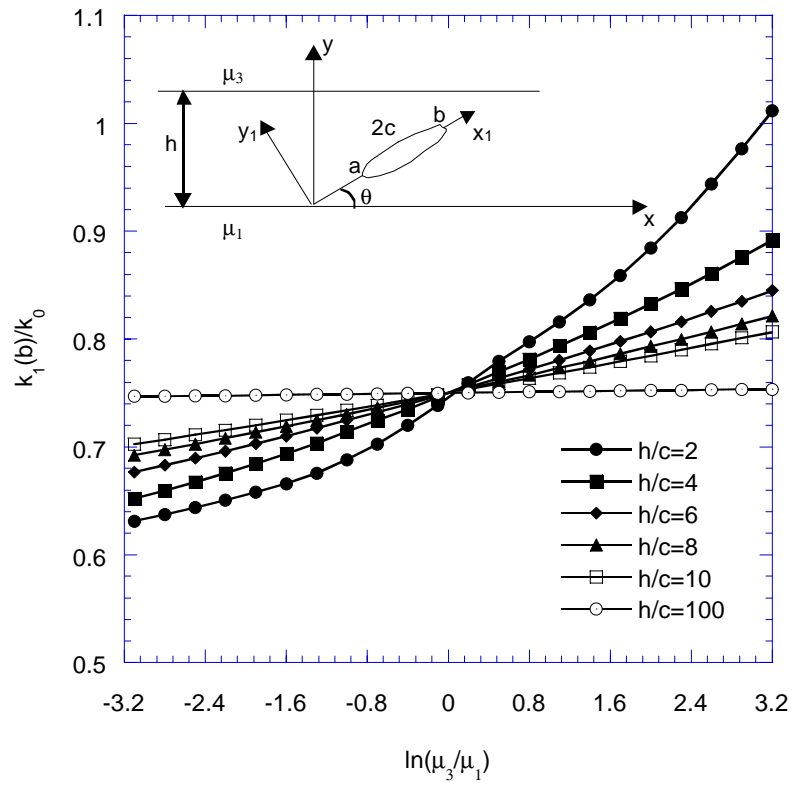


Figure 5. Normalized mode I SIF at crack tip (b) for various h/c , $\theta=30$ deg. and center of the crack is located at $h/2$, under loading of uniform normal stress.

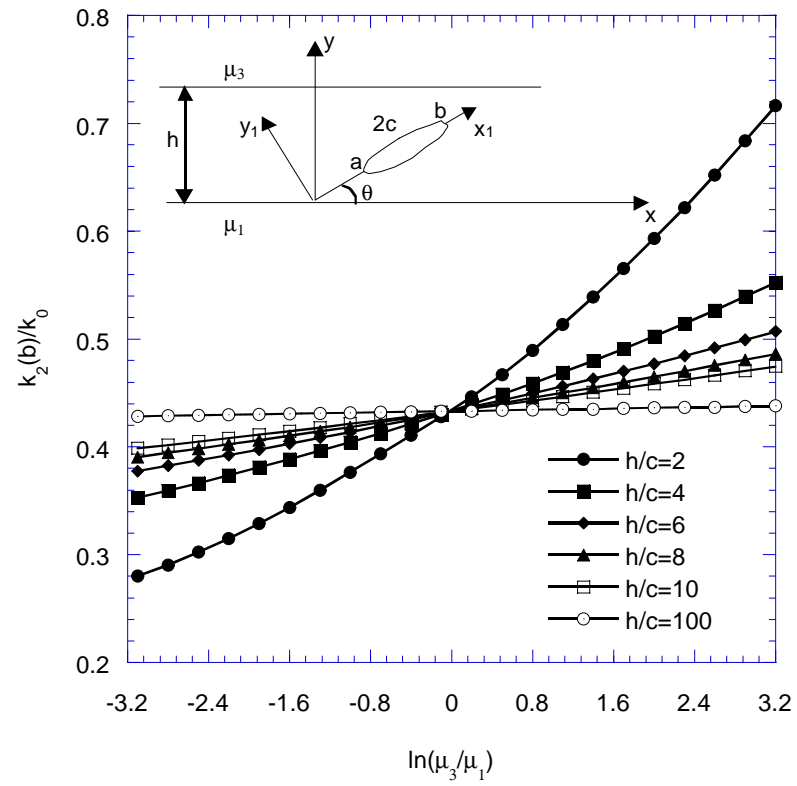


Figure 6. Normalized mode II SIF at crack tip (b) for various h/c , $\theta=30$ deg. and center of the crack is located at $h/2$, under loading of uniform normal stress.

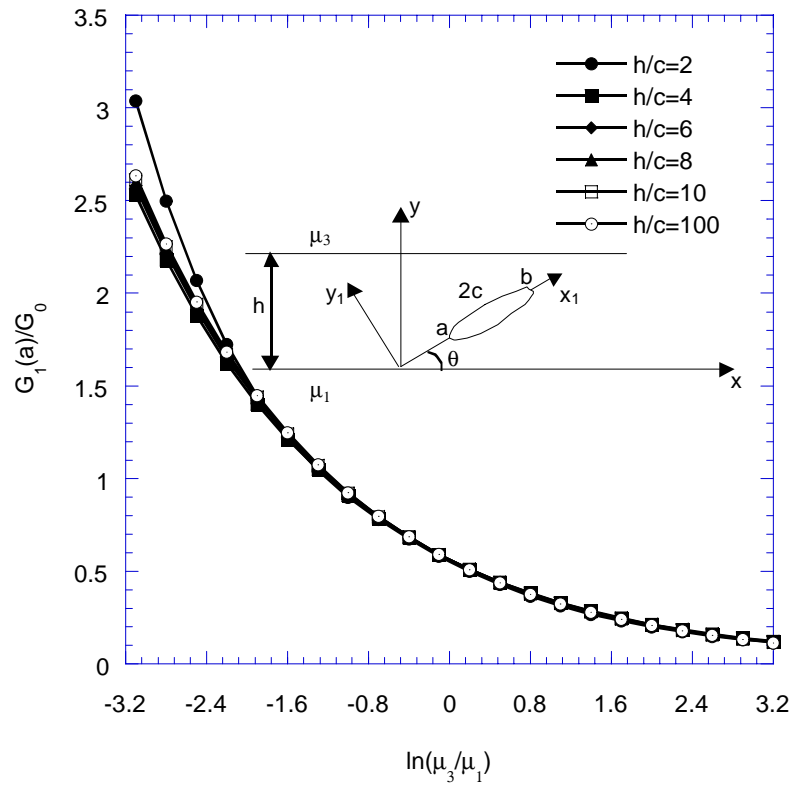


Figure 7. Normalized mode I SERR at crack tip (a) for various h/c , $\theta=30$ deg. and center of the crack is located at $h/2$, under loading of uniform normal stress.

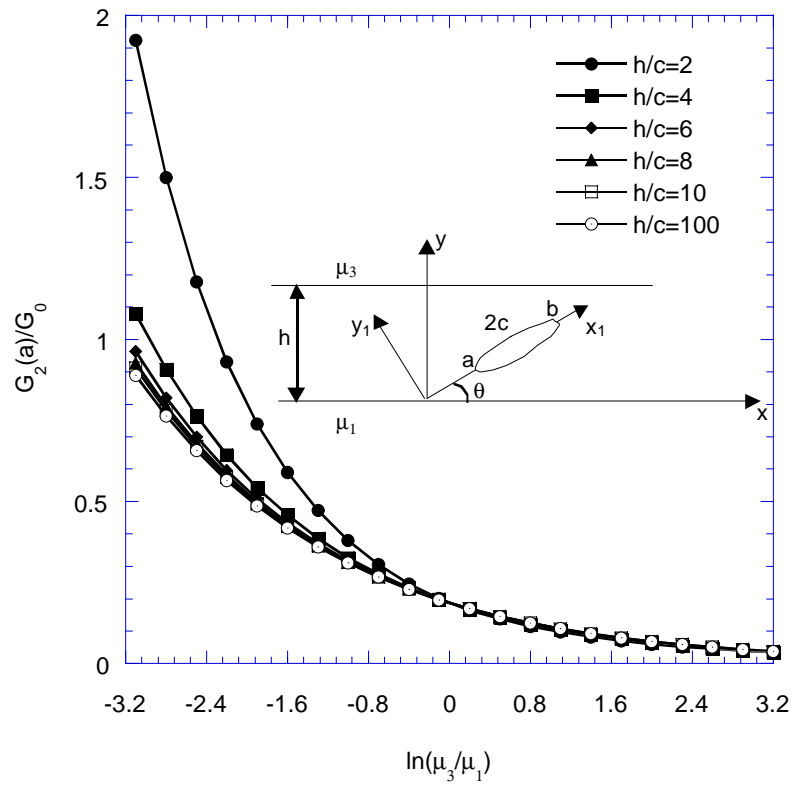


Figure 8. Normalized mode II SERR at crack tip (a) for various h/c , $\theta=30$ deg. and center of the crack is located at $h/2$, under loading of uniform normal stress.

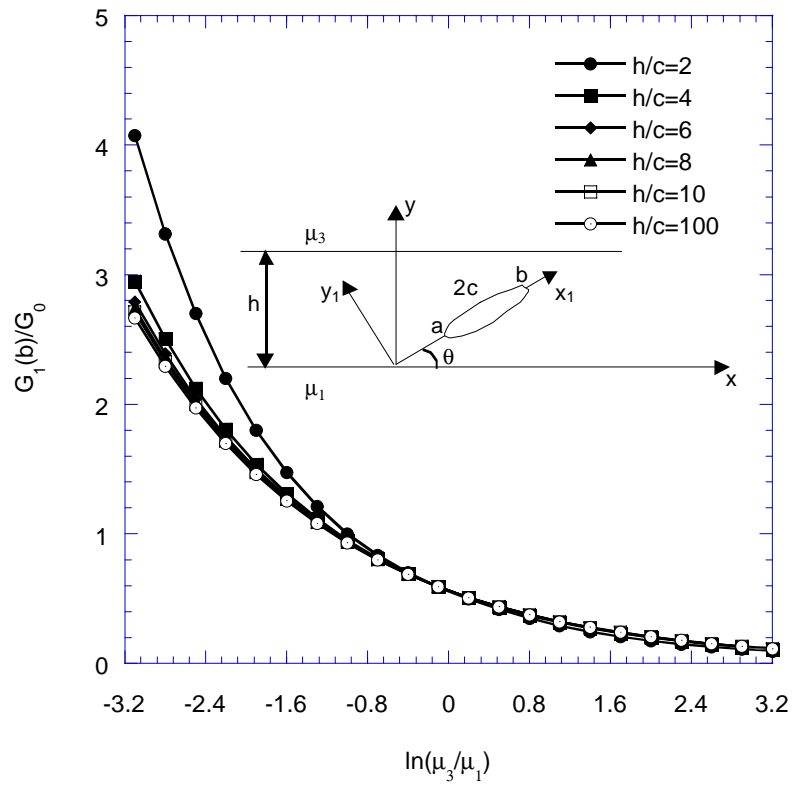


Figure 9. Normalized mode I SERR at crack tip (b) for various h/c , $\theta=30$ deg. and center of the crack is located at $h/2$, under loading of uniform normal stress.

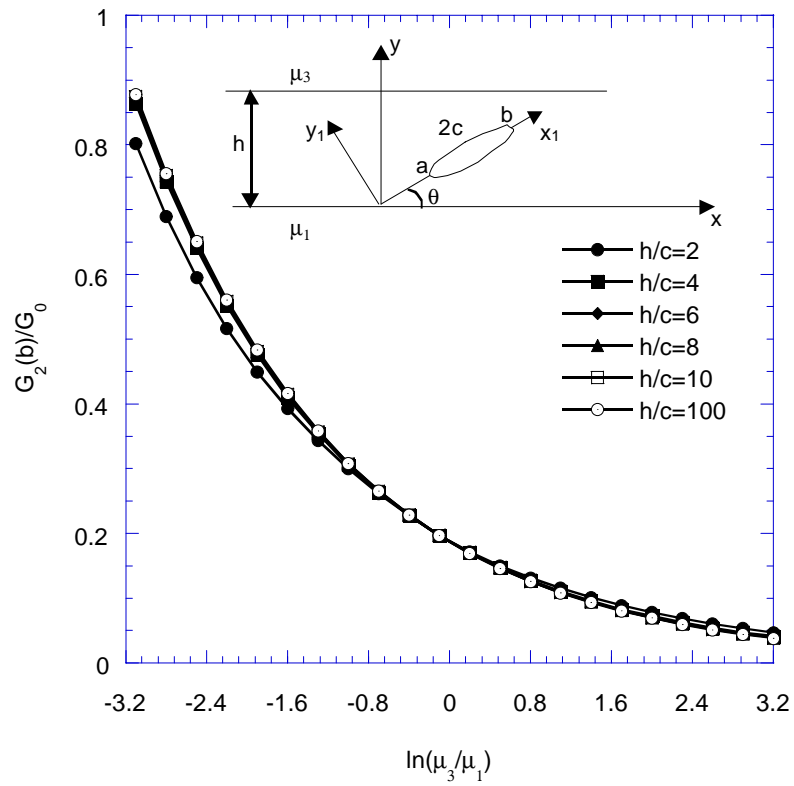


Figure 10. Normalized mode II SERR at crack tip (b) for various h/c , $\theta=30$ deg. and center of the crack is located at $h/2$, under loading of uniform normal stress.

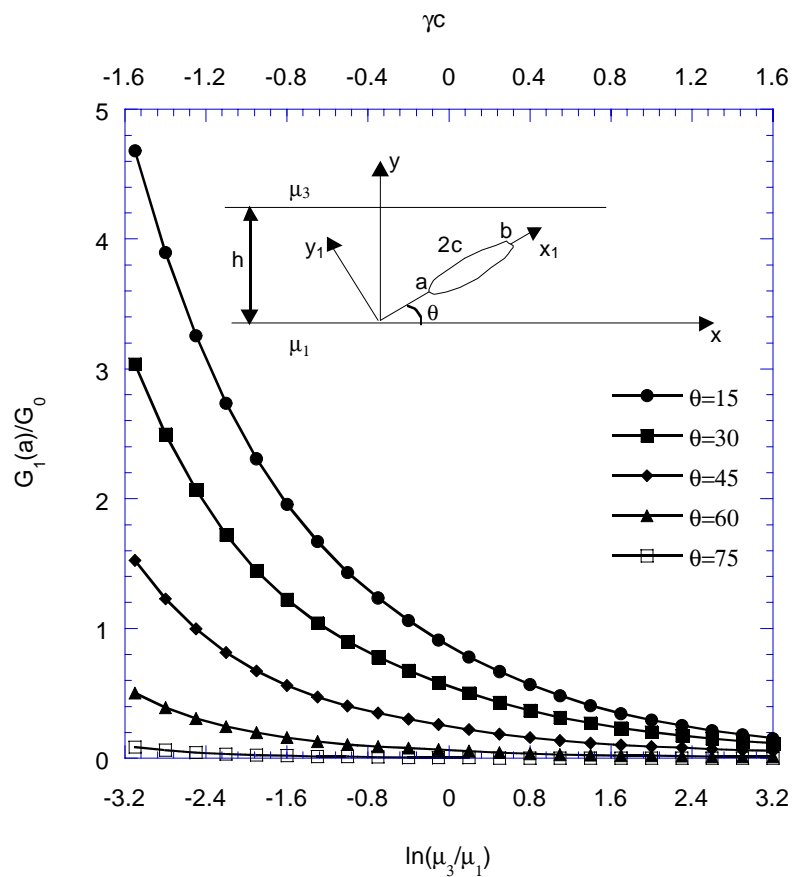


Figure 11. Normalized mode I SERR at crack tip (a) for various θ , $h/c=2$ and center of the crack is located at $h/2$, under loading of uniform normal stress.

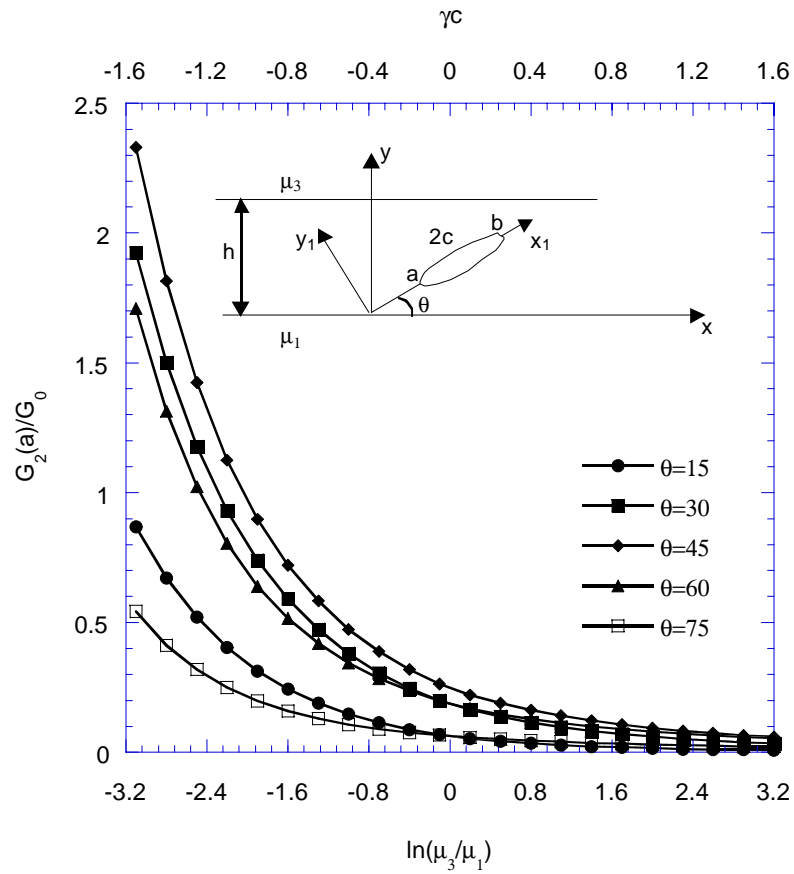


Figure 12. Normalized mode II SERR at crack tip (a) for various θ , $h/c=2$ and center of the crack is located at $h/2$, under loading of uniform normal stress.

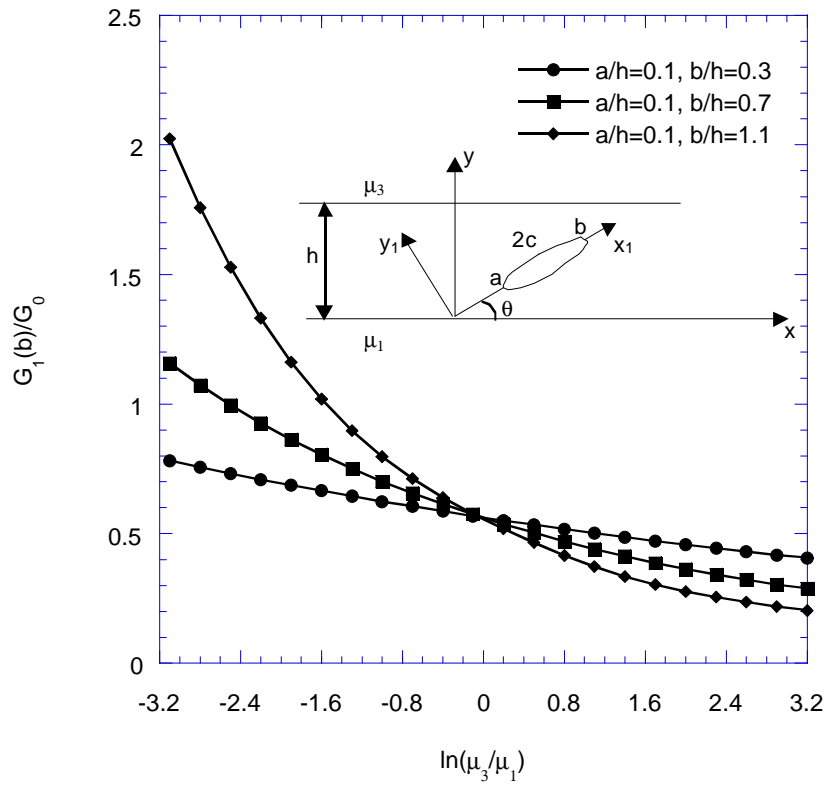


Figure 13. Normalized mode I SERR at crack tip (b) for $\theta=30$ deg., same h and fixed crack tip (a) and movement of crack tip (b), under loading of uniform normal stress.

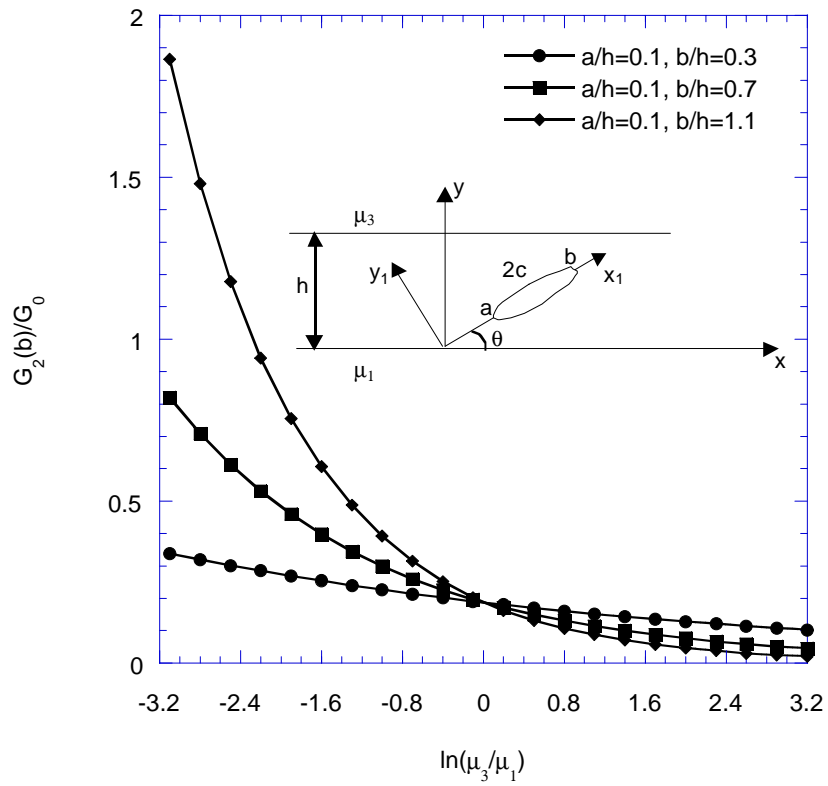


Figure 14. Normalized mode II SERR at crack tip (b) for $\theta=30$ deg., same h and fixed crack tip (a) and movement of crack tip (b), under loading of uniform normal stress.

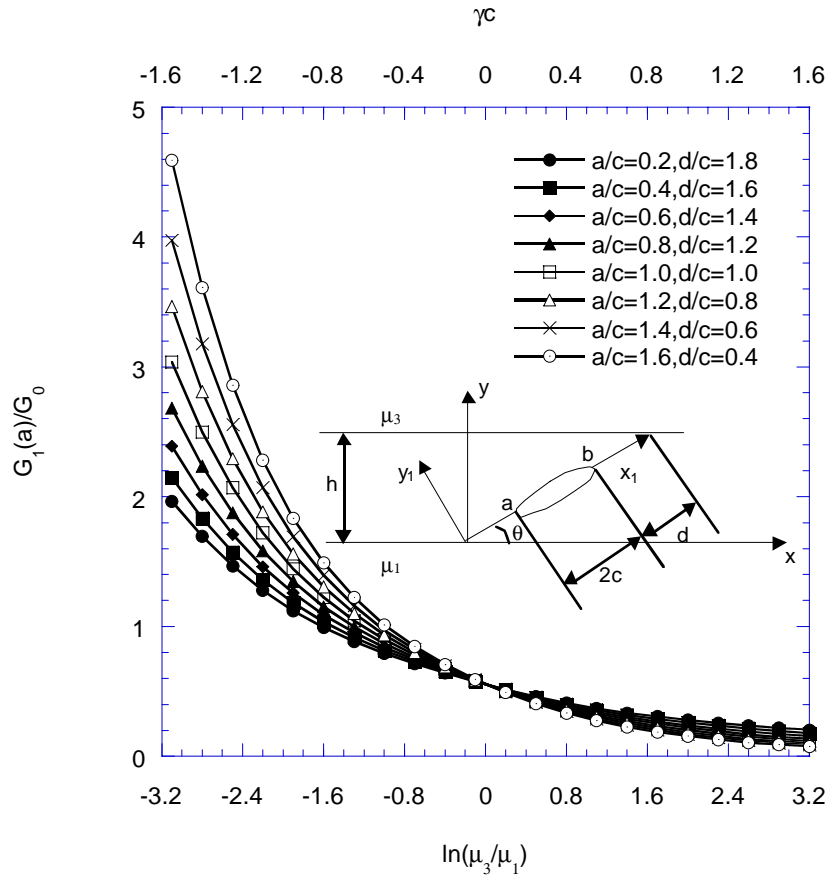


Figure 15. Normalized mode I SERR at crack tip (a) for $\theta=30$ deg., $h/c=2$, constant crack length and various positions of crack, under loading of uniform normal stress.

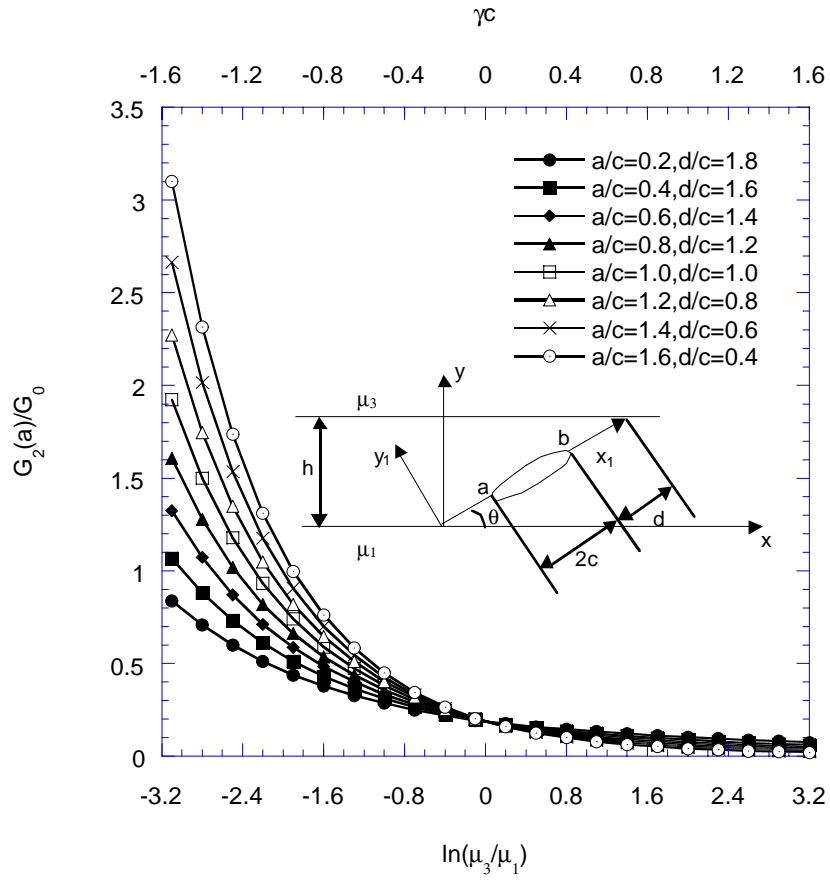


Figure 16. Normalized mode II SERR at crack tip (a) for $\theta=30$ deg., $h/c=2$, constant crack length and various positions of crack, under loading of uniform normal stress.

REPORT DOCUMENTATION PAGE			Form Approved OMB No. 0704-0188	
Public reporting burden for this collection of information is estimated to average 1 hour per response, including the time for reviewing instructions, searching existing data sources, gathering and maintaining the data needed, and completing and reviewing the collection of information. Send comments regarding this burden estimate or any other aspect of this collection of information, including suggestions for reducing this burden, to Washington Headquarters Services, Directorate for Information Operations and Reports, 1215 Jefferson Davis Highway, Suite 1204, Arlington, VA 22202-4302, and to the Office of Management and Budget, Paperwork Reduction Project (0704-0188), Washington, DC 20503.				
1. AGENCY USE ONLY (Leave blank)		2. REPORT DATE October 1999		3. REPORT TYPE AND DATES COVERED Final Contractor Report
4. TITLE AND SUBTITLE Analysis of a Generally Oriented Crack in a Functionally Graded Strip Sandwiched Between Two Homogeneous Half Planes			5. FUNDING NUMBERS WU-537-04-22-00 NAG3-2069	
6. AUTHOR(S) N. Shbeeb, W.K. Binienda and K. Kreider				
7. PERFORMING ORGANIZATION NAME(S) AND ADDRESS(ES) The University of Akron Akron, Ohio 44325-3905			8. PERFORMING ORGANIZATION REPORT NUMBER E-11760	
9. SPONSORING/MONITORING AGENCY NAME(S) AND ADDRESS(ES) National Aeronautics and Space Administration John H. Glenn Research Center at Lewis Field Cleveland, Ohio 44135-3191			10. SPONSORING/MONITORING AGENCY REPORT NUMBER NASA CR-1999-209166	
11. SUPPLEMENTARY NOTES Project Manager, Gary R. Halford, Research and Technology Directorate, NASA Glenn Research Center, organization code 5000, (216) 433-3265.				
12a. DISTRIBUTION/AVAILABILITY STATEMENT Unclassified - Unlimited Subject Category: 39 This publication is available from the NASA Center for AeroSpace Information, (301) 621-0390.			12b. DISTRIBUTION CODE	
13. ABSTRACT (Maximum 200 words) The driving forces for a generally oriented crack embedded in a Functionally Graded strip sandwiched between two half planes are analyzed using singular integral equations with Cauchy kernels, and integrated using Lobatto-Chebyshev collocation. Mixed-mode Stress Intensity Factors (SIF) and Strain Energy Release Rates (SERR) are calculated. The Stress Intensity Factors are compared for accuracy with previously published results. Parametric studies are conducted for various nonhomogeneity ratios, crack lengths, crack orientation and thickness of the strip. It is shown that the SERR is more complete and should be used for crack propagation analysis.				
14. SUBJECT TERMS Functionally graded materials; Stress intensity factors; Strain energy release rate; Mixed-mode; Crack			15. NUMBER OF PAGES 55	
			16. PRICE CODE A04	
17. SECURITY CLASSIFICATION OF REPORT Unclassified	18. SECURITY CLASSIFICATION OF THIS PAGE Unclassified	19. SECURITY CLASSIFICATION OF ABSTRACT Unclassified	20. LIMITATION OF ABSTRACT	